Lower Passaic River

System Understanding of Sediment Transport

May, 2011

Prepared by

Sea Engineering, Inc

and

HDR|HydroQual, Inc

CONTENTS

List of Figures 2
Introduction 5
System Overview 5
Estuarine Circulation and River Flow 6
Sediment Transport 8
Transport Characterization 9
Water Column 9
Chant 2004/2005 9
Summer 2009 Measurements 10
Fall 2009MEasurements 10
Sediment Flux vs. Flow Rate 11
Mass Balance 11
Morphology 12
Bathymetric Change 12
Pilot Dredging Bathymetric Change 13
Morphologic Features 14
Sediment Bed 15
Newark Bay 17
March 2010 High Flow Event 17
Summary 18
References 20

LIST OF FIGURES

Figure 1. Map of the Lower Passaic River region (MPI, 2007). 22
Figure 2. Conceptual diagram of processes related to sediment and contaminant transport. 23
Figure 3. Variation in river cross-sectional area with river mile numbered from river mile 0 at the mouth (MPI, 2007). 24
Figure 4. Timeline showing the times of coring (top) and mooring deployments (bottom) from the Sommerfield and Chant study (2010). Passaic River discharge at Little Falls and salinity data in psu are shown for reference. KBK=Kill Van Kull mooring, NB=Newark Bay. 25
Figure 5. Estuarine processes active in the Lower Passaic River, a partially mixed estuary. 26
Figure 6. Time series of combined tidal (red) and tidally filtered velocities (blue) from the LPR hydrodynamic model (HQI, 2008), in the tidal fresh region (upper panel) and the estuarine region (lower two panels). Positive velocities are in the flood direction (upstream) and negative velocities are in the ebb direction (downstream). 27
Figure 7. Conceptual contribution of three forcing factors relevant to transport in the Lower Passaic River. The figure represents median flow conditions at Dundee Dam. 28
Figure 8. Conceptual contribution of three forcing factors relevant to transport in the Lower Passaic River. The figure represents elevated flow conditions at Dundee Dam. 29
Figure 9. Location of high tide salt front as a function of flow rate determined from the HQI hydrodynamic model (MPI, 2007). 30
Figure 10. Estuarine and sediment transport processes active in the Lower Passaic River. 31
Figure 11. Longitudinal profiles of salinity and TSS from Chant (2009) corresponding to 1 and 330 m^3/s river flow rates respectively. 32
Figure 12. Longitudinal profiles of TSS (top) and salinity (bottom) during low flow conditions in September 8th, 2004 from preliminary HQI hydrodynamic and sediment transport model. 33
Figure 13. Tidally averaged velocity profile during low flow conditions in August 2004 from preliminary HQI hydrodynamic and sediment transport model. The profile is located at river mile 5. Negative velocity is directed downstream. 34
Figure 14. Time series profiles of salinity (red lines are surface and blue lines are bottom of the water column) and TSS (solid contours) near RM 3 from Chant et al. (2009) corresponding to high and low river flow rates respectively. 35
Figure 15. Sediment transport (positive is upstream) as a function of tidal range and river discharge (flow rate) estimated from current meter and backscatter measurements near RM 3 (Chant et al., 2009). 36
Figure 16. LPR flow rate and local precipitation during the summer 2009 instrument deployment (top panel). The instantaneous and daily averaged sediment fluxes are calculated for Station 1 (bottom panels). 37
Figure 17. LPR flow rate and local precipitation during the fall 2009 instrument deployment (top panel). The instantaneous and daily averaged sediment fluxes are calculated for the RM 4.2 mooring (bottom panels). 37

Figure 18. Daily averaged sediment flux as a function of river flow rate. The data is a combination of the stations between RM 3 and 4.2 from the Chant et al. (2009), Summer 2009 (OSI, 2009), and CPG Fall 2009 PWCM datasets and the data fit. 38
Figure 19. Sediment balance during low and elevated river flow periods. The size of each component is relative to the contribution of each term in the balance. 39
Figure 20. Flow rate and estimated cumulative transport near RMs 3 to 4.2 (top) and cumulative river input from Dundee Dam. Estimated transport near RMs 3 to 4.2 (bottom) from October 1994 through January 2010. 40
Figure 21. Daily water column sediment transport (negative is upstream) as a function of flow rate at 8 river mile stations in the Lower Passaic calculated from the preliminary HQI hydrodynamics and sediment transport model. 41
Figure 22. Depth of the river channel based on a 2004 bathymetric survey as well as the original dredged elevations as reported in USACE records. 42
Figure 23. Estimated depths of the river channel from Chant et al. (2009). 43
Figure 24. Bathymetric change from 1989 to 2004 from conditional simulations (LB, 2010). 44
Figure 25. Pre- and Post-surveys for the 2005 pilot dredging operations. 45
Figure 26. Net change in bed elevation following pilot dredging operations. Intervals for each change comparison are listed in the plot legend. 46
Figure 27. Shaded multibeam data and contours from the 2008 survey and an overlay of qualitatively identified morphologic regions near RM 2. 47
Figure 28. Shaded multibeam data and contours from the 2008 survey and an overlay of qualitatively identified morphologic regions near RM 4. 48
Figure 29. Shaded multibeam data and contours from the 2008 survey and an overlay of qualitatively identified morphologic regions near RM 6. 49
Figure 30. Shaded multibeam data from the 2008 survey highlighting bed features near RM 2.7 (left) and RM 8.3 (left). 50
Figure 31. Side scan bottom texture identification from RM 0-6 and 8-12. 51
Figure 32. Side scan bottom texture identification from near RM 8. 52
Figure 33. Interpolated surfaces of percent fines developed from the 2005 and 2009 surface sediment samples. 53
Figure 34. Locations of the three upper river 2005 CSM cores. 54
Figure 35. Locations of the two lower river 2005 CSM cores. 55
Figure 36. Profiles of Cs-137 for the 5 2005 CSM cores with 1995 PCB profiles overlain. 56
Figure 37. Shaded multibeam data from the 2008 survey and SPI camera deposition depths with photos at RM 3.9. 57
Figure 38. Map of 16 Sedflume core locations on the LPR. Note that two collocated cores were collected within ~10m of each location. 58
Figure 39. Average sediment erosion rate ratios for Sedflume core locations P01 through P15 colored by morphologic regions. 59
Figure 40. Longitudinal cross section of TSS derived from measurements by R. Chant during the March 16, 2010 high flow event. 60
Figure 41. Comparison of channel features in the 2008 and 2010 multibeam datasets in the vicinity of the pilot dredge region. 61
Figure 42. Comparison of channel features in the 2008 and 2010 multibeam datasets. 62

Figure 43. Comparison of channel features in the 2008 and 2010 multibeam datasets. The figure shows the evolution of bedforms. 63
Figure 44. Conceptual diagram of key processes during low river flow conditions. 64
Figure 45. Conceptual diagram of key processes during high river flow conditions. 65

Lower Passaic River

System Understanding of Sediment Transport

INTRODUCTION

Historically, the Lower Passaic River (LPR) below Dundee Dam (Figure 1) has been contaminated with a range of Contaminants of Potential Concern (COPCs). Many of these contaminants are hydrophobic and therefore strongly sorb to sediments, and in particular, fine-grain organic material in the system. Over time the accumulation of these contaminated sediments has resulted in a persistent COPC signal in the LPR that is of environmental concern. Since the most significant transport pathway for these hydrophobic COPCs is by transport of the sediments to which they are sorbed, sediment transport is a key system wide process to understand when evaluating environmental risk and any remedial selection.

In the most basic terms, sediment transport begins with the erosion, or mobilization, of sediment from one location where there is relatively high energy (e.g. watershed, river bed) due to currents, waves, and anthropogenic activities (e.g. ship propeller scour). Once mobilized, the sediment is transported in the water column to a location where there is less energy where it deposits out of the water column and comes to rest. While mobilized, contaminated sediments not only carry the mass of contaminants sorbed to them, but also potentially desorb contaminants as they move in the water column; therefore, the sediment transport processes are critical to fully understanding contaminant fate and transport in a system. In addition, physical and biological processes can release contaminated pore water from the sediment bed. Figure 2 shows a conceptual diagram of these transport processes. These processes are highly non-linear in their frequency and interaction and require a robust qualitative and quantitative description.

The objective of this document is to outline a basic System Understanding for Sediment Transport (SUST) which provides a description of the sediment transport processes governing the fate and transport of contaminants in the LPR. Although a Conceptual Site Model (CSM) has been developed as part of a Focused Feasibility Study of the Lower 8 Miles of the LPR, the system understanding will be used as a tool for synthesizing and linking existing data sets and sediment transport modeling analysis for answering site management questions. Additionally, the understanding will be used to develop a strategy to guide future data and sediment transport modeling analysis efforts in addressing the site management questions. The conceptual understanding presented here is primarily qualitative in nature and is not intended to present a complete analysis of all data available for the system.

SYSTEM OVERVIEW

The LPR and its watershed, including Saddle River, Second River, and Third River, define the Study Area of the Lower Passaic River Restoration Project. The LPR waterway is bounded by Dundee Dam (River Mile [RM] 17.4) upstream and Newark Bay (RM 0) downstream. River depths throughout the LPR range from less than 1 m (3.3 ft) in the upper portion to almost 10 m (32.8 ft) in the lower portion of the LPR. Figure 3 shows the significant upstream decrease in cross sectional area with river mile. Flow over Dundee Dam is the primary source of freshwater and solids to the LPR. Table 1 illustrates the median

flow and recurrence intervals of flow rates on the river. Additionally, the mouth of the river in Newark Bay is driven by a semi-diurnal tidal water level with a range of approximately 1.5 m (4.9 ft).

Table 1. Median flow and recurrence intervals for river flow on the LPR.

Return Period	Little Falls (cfs)	Little Falls (m^3/s)
Median	610	17
1-month	3900	110
6-month	4500	127
1-year	6200	175
2-year	6751	191
5-year	9968	282
10-year	12219	346
25-year	15280	432
50-year	17465	494
100-year	19808	561

Salinity in Newark Bay is high relative to the freshwater inflow over Dundee Dam, especially in the bottom waters, but it varies in response to freshwater flow and wind (Chant et al., 2009). Sommerfield and Chant (2010) conducted extensive moored measurements of hydrodynamics from 2007 to 2009 in Newark Bay. Figure 4 shows a time series of LPR flow rate and salinities in the mouth of the Passaic River and Newark Bay. During low flow periods the salinity in Newark Bay is over 20 psu (or ppt), whereas the salinities at the mouth of the LPR are typically 5 psu lower than Newark Bay. The salinity drops significantly at both stations as the river flow increases. The effects of salinity variations on circulation are discussed in the following section.

ESTUARINE CIRCULATION AND RIVER FLOW

The density contrast between the freshwater inflows from the river and the saltier water in Newark Bay interacts with the tides to form a *partially mixed estuary* (Dyer, 1997). The heavier saltwater in Newark Bay tends to drive under the outgoing river water creating a salinity (and density) stratified water column throughout the lower few miles of the river (vertical curved black line in Figure 5). At the same time, strong tidal currents (flooding into the river or ebbing out of it) generate turbulence that partially mixes the water column. The constantly adjusting balance between river inflow, salinity at the river mouth, and tidal mixing determines the extent of salt intrusion into the river and the structure of the two layer *estuarine circulation*. The net inflow on the bottom and net outflow at the surface typical of a partially mixed estuarine circulation are shown schematically in Figure 5.

The net tidal current energy gradually decreases as the tide moves up the Passaic River, primarily due to decreasing upstream intertidal volume approaching Dundee Dam and frictional losses. However, the tidal current energy tends to decrease due to decreasing tidal prism while it is also concentrated by the upstream narrowing and shallowing cross-section of the river bed. As a result, flood and ebb tidal currents are significant contributors to currents in much of the river. Local combinations of tidal, riverine,

and estuarine flow vary both up the river and across its width, generating strong asymmetries in near bottom flow that largely control the direction and magnitude of sediment transport.

A 3-dimensional hydrodynamic model of the LPR was developed and validated which provides additional insight into the circulation in the LPR (HQI, 2008). Time-series of combined tidal and net axial flow velocities above (tidal fresh) and below (estuarine) the limit of salt intrusion from the LPR model are shown in Figure 6. In this modeled case the river flow is held constant but the tide varies over a fortnightly cycle to illustrate the effects of the spring-neap cycle of tidal energy. In the tidal fresh river the largest instantaneous velocities are during ebb tide because the ebb tides and river currents combine to provide larger overall velocities. Below the salt front the estuarine circulation and flood tides add constructively, such that the net flow is in the upstream direction during flood tide. The estuarine circulation during neap tide is generally stronger than the spring tide because there is less tidal current and mixing. The lower mixing allows for stronger salinity stratification which results in a greater exchange flow. In the surface layer, downstream of the salt front, tidally-averaged flows are always seaward and are stronger than in the tidal fresh river due the confinement of the downstream flow in the surface layer and entrainment of salt water from the lower layer. Different ratios of river flow to estuarine circulation change the relative magnitudes of the flow in different regions, but the general pattern of strongest flows during ebb tide in the river and the estuarine upper layer, and during flood tide in the estuarine lower layer, is almost always present.

To better illustrate the physical processes controlling hydrodynamics and sediment transport in the Passaic River, it is useful to examine the relative energy levels of different flow components in each portion of the LPR. As mentioned, the key forcing factors are the river flow, the estuarine circulation associated with salt intrusion, and tidal fluctuations. Additionally, wave action in the wide and shallow Newark Bay can strongly influence sediment resuspension over the shoals and subsequent transport into the LPR during flood tides. Figure 7 shows the typical situation where the river flow dominates the upper river beyond the reach of the saltwater front. This region is labeled “River Dominant”. In the tidal mid-river, the interactions between tidal currents, river flow, and estuarine circulation described above control spatial patterns in flow and sediment transport near the salt front. The region where the freshwater and saltwater interact is labeled “Mixed”. Downstream of this region, where the water column is vertically stratified, is considered “Estuary Dominant”. Wave energy is most important outside the mouth of the river, but its influence can extend slightly into the river through its effect on suspended sediment levels in Newark Bay. Figure 8 illustrates how this scenario changes as the river flow increases. At higher river flows the salt intrusion is pushed downstream and potentially out of the river. Most of the river is dominated by strong downstream flow interacting with the tide in the lower river. The locations of the regions in these figures are for conceptual illustration and are not meant to be quantitative.

To characterize the extent of the saltwater/freshwater interaction, it is useful to define a “Salt Front”. For the purposes of the CSM (MPI, 2007), this was defined as the location where the salinity at the bottom of the water column drops below 0.5 psu. Figure 9 presents LPR model output from the simulation period of March 1995 through September 2004. The daily location of the salinity concentration of 0.5 psu at high tide is plotted against the upstream flow rate. There is a strong relationship between river flow rate and salt front location. The median flow of 17 m^3/s (610 cfs) from Table 1 puts the high tide salt front at approximately RM 8. As the river flow rate increases the 0.5 psu salt front is pushed out to the lower two miles of the river. Conversely, in extremely low flow conditions the salt front can reach to RM 14 and

above. One can similarly scale the upstream reach of the mixed energy zone in Figures 6 and 7 with this plot. It is noted that the 0.5 psu functional definition of the salt front used in the CSM is based on a chemical definition. Sediment transport analyses often use a value of 2 psu, based on physical observations of the location of the estuarine turbidity maximum (ETM) zone. The 2 psu definition would generally have the effect of shifting the results presented here downstream slightly.

SEDIMENT TRANSPORT

The dynamic between river dominant behavior in the upper river, estuarine circulation in the lower river, and tidal currents that gradually decrease with distance upstream, provides a complex interplay of processes governing sediment transport in the LPR. Dundee Dam plays a critical role in these processes. Dundee Dam not only regulates the dominant flow through the system, but also provides a large source of sediment to the system. The upper river generally behaves as a normal river with advective transport of sediments downstream.

During low flow conditions, the tidally generated currents typically resuspend some sediment during peak flood and ebb flows, which then settle back out during slack tides (i.e. lowest velocities). The amount of surface sediment suspended and deposited during these tidal cycles is typically on a scale of a few millimeters (Sanford, 1992). The net transport of this tidally resuspended sediment is typically very slow, yet the estuarine circulation during low flow largely controls where the sediment goes. As discussed, the combination of the river flow, salinity gradient, and tidal energy in the reach downstream of the salt front result in a residual upstream flow near the bottom. The zone of convergence between sediment being carried upstream from the direction of Newark Bay in the lower layer and the sediment load moving downstream from the river creates a region of increased sediment concentrations in the water column. This zone of elevated sediment concentrations in the water column is called the Estuarine Turbidity Maximum (ETM), and plays a key role in estuarine sediment transport. The bathymetric data in systems comparable to the LPR suggest that over the long term (i.e. decadal time scales), the ETM is a region of sediment accumulation; although, periodic high river flow and storm events (e.g. Nor'easters, tropical storms) can cause short term changes in this pattern (Geyer et al., 2000). Downstream of the ETM in the deeper waters of the navigation channel are lower bed shear stress regions that will have higher probabilities of deposition. These areas have also shown long term net accumulation. Figure 10 presents a conceptual diagram of the sediment transport processes at work in the LPR during low flow conditions.

During higher river flows, the zone of estuarine circulation moves downstream and the system is dominated by the strong downstream river flow. The high flows can cause sediment erosion in higher shear regions of the river (e.g. outer bends and constrictions) and deposition of the resuspended sediment in lower shear regions (e.g. inner bends). During these events, the net sediment transport is out of the LPR into Newark Bay as will be shown from data in the following sections.

The following sections will illustrate the transport processes in more detail with field and modeling results.

TRANSPORT CHARACTERIZATION

The following sections extend a more detailed picture of the processes in the LPR based on data and modeling. The goal is to present a more detailed description of the river processes and provide general summary of available data.

WATER COLUMN

Much of the discussion in the previous section dealt with hydrodynamic and sediment transport processes in the water column due to river and tidal flows and estuarine circulation. A few key data sets and analyses provide excellent illustration and quantification of the water column processes. The studies outlined here are the Chant 2004/2005 (Chant et al. 2009), Summer 2009 (OSI, 2009), and Cooperating Parties Group (CPG) Fall 2009 Physical Water Column Monitoring (PWCM) program data collection efforts. By collating these studies a more complete picture of processes in the water column can be developed.

CHANT 2004/2005

The study implemented by R. Chant at Rutgers University in 2004 and 2005 provide an excellent baseline of water column velocity, salinity, and Total Suspended Solids (TSS) measurements in the LPR. The study is summarized in a 2009 paper (Chant et al., 2009). Longitudinal profiles of salinity and TSS during low and high flow cases illustrate the dominance of estuarine and riverine processes depending on flow. The top panel of Figure 11 shows a low flow condition of approximately 1 m^3/s (35 cfs), well below the median flow rate on September 8th, 2004. The salt front extends to between RM 10 and 12 with an ETM evident at the salt front. The ETM has measured TSS values of up to 50 mg/L. The range of the salt front is consistent with the conceptual model presented in Figure 7 for very low flows. The development of the turbidity maximum at the salt front illustrates that the LPR behaves consistently with our conceptual model of estuarine circulation.

Conversely, the bottom panel of Figure 11 shows measurements conducted when the river flow was 330 m^3/s (11653 cfs), greater than a 1-in-5 year flow. The 2 ppt salt front is pushed out into Newark Bay with high solids levels (above 100 mg/L) well into Newark Bay and concentrations exceeding 250 mg/L at RM 0. These measurements illustrate a case where the river flow dominates the entire LPR and there is a strong export of sediment out of the mouth of the river.

Preliminary hydrodynamic and sediment transport modeling conducted by HQI predicted similar behavior in the river. Figure 12 shows longitudinal profiles of TSS and salinity during simulations of the low flow period on September 8th, 2004. The salt front (bottom panel) extends to approximately RM 7 at high tide and recedes to RM 3 during low tide. The TSS shows a turbidity maximum near the salt front at RM 7. Figure 13 shows the tidally averaged velocity profile at RM 5. The profile shows a clear residual upstream velocity near the bottom and strong downstream velocity near the surface. The profiles of the salt front, TSS, and the residual velocity help to illustrate the magnitude and extent of estuarine circulation.

Time series profiles of salinity and total suspended solids from moorings deployed during the Chant et al. (2009) study provide a detailed picture of the water column structure in the lower river. Figure 14 shows Acoustic Doppler Current Profiler (ADCP) and TSS measurements at approximately RM 3 corresponding to high (top) and low (bottom) river flow rates. During the high flow period, a significant decrease in salinity during ebb tide (red and blue lines) is accompanied by a large increase in TSS (solid contours). The data show a high TSS during ebbing tides denoting a strong downstream transport of sediment during this elevated flow event. The low flow period (bottom) shows reduced TSS levels and a strong diurnal salinity signal. During this normal period of estuarine circulation the TSS levels are higher on flood tide than ebb tide denoting a net upstream transport of solids.

Chant et al. (2009) calculated the daily average fluxes at the mooring near RM 3 (Figure 14) over approximately 7 months of measurement in 2004 and 2005 using the velocity and TSS measurements. Figure 15 shows a summary of the flux data as a function of tidal range and river discharge (flow rate). The hotter (e.g. orange) colors denote net upstream transport while the cooler colors (e.g. blue) denote net downstream transport. The summary of data shows that as river flow drops, estuarine circulation is responsible for the upstream transport of solids at the mooring location. As the river flow increases, the estuarine circulation is disrupted and the net flux of sediment is downstream.

SUMMER 2009 MEASUREMENTS

Moored ADCP current velocity data and turbidity data were collected by Ocean Surveys, Inc. (OSI, 2009) for Tierra Solutions, Inc. (TSI) at three stations between July 23rd and September 1st, 2009. The three stations were located at RMs 4.1 (Station 1), 3.2 (Station 2), and 2.1 (Station 3) of the river. To obtain water column profiles of TSS at each station, TSS was computed from ADCP echo intensity data. Additional ADCP transect data were collected by OSI during 21 measurement events between July 25th and 31st, 2009 to determine the instantaneous cross channel discharge and sediment flux at each of the three stations. All of the data analysis presented here is considered preliminary and for qualitative evaluation only.

The total discharge and sediment flux computed from the transects can be correlated to the velocity and TSS profile for the mooring at that location for each individual transect time. The correlation can then be applied to the time-series of the mooring to obtain a continuous flux relationship for each transect location. The correlation allows the visualization of daily averaged fluxes similar to the Chant et al. (2009) calculations. Figure 16 shows the data for Station 1 during the summer deployment. The flow rates were generally elevated above the median flow of 17 m^3/s (610 cfs). The second and third panels show the instantaneous sediment flux, which clearly shows the tidal signal, and the daily averaged sediment flux. The daily averaged flux shows upstream sediment flux during the lowest flow period and downstream flux during the stronger downstream river flows. The behavior observed in these measurements is consistent with the system understanding.

FALL 2009MEASUREMENTS

Moored ADCP current velocity and turbidity data were collected by OSI in 2009 for the CPG at five stations between October and December 2009. The five stations were located at RMs 1.4, 4.2, 6.7, 10.2, and 13.5. As with the summer dataset, water column profiles of TSS were computed from ADCP echo intensity data. Additionally, six transecting events were conducted by OSI between October 12th and December 15th, 2009 to determine the instantaneous cross channel discharge and sediment flux at each of

the five stations. Six transects were conducted at each station location (two per month) for a total of 30 transects.

As with the summer dataset, the total discharge and sediment flux computed from the transects can be correlated to the velocity and TSS profile for the mooring at that location to determine daily averaged fluxes. Figure 17 shows the data for Station 1during the fall deployment. The flow rates were generally elevated during two peak events with one event reaching over 100 m^3/s (3530 cfs). The second and third panels show the instantaneous sediment flux and the daily averaged sediment flux. The daily averaged flux shows stronger upstream sediment flux during the low flow periods before the events, and downstream flux during the stronger downstream river flows. The behavior observed in these measurements is again consistent with the system understanding.

SEDIMENT FLUX VS. FLOW RATE

All of the flux data from the three measurement events can be collapsed into daily sediment flux as a function of river flow rate, a technique adapted from the Chant et al. (2009) analysis. The curve in Figure 18 illustrates that at river flow rates below approximately 20 m^3/s (706 cfs) the net sediment transport through RMs 3 to 4.2 is upstream. Above 20 m^3/s (706 cfs), river flow begins to dominate the signal and the net sediment transport is downstream. At high river flows (greater than ~ 200 m^3/s or 7063 cfs) the net downstream transport is over 100 times higher than the upstream transport during low flow, however these events occur during a much shorter time frame. It is important to note that this analysis is limited in that it is based on correlations to limited measurements at three locations within RMs 3 to 4.2 in the river which could introduce error into the absolute flux at a specific location.

MASS BALANCE

Using the transport information, a conceptual mass balance in the river can be constructed. Generally, the mass balance in the river can be defined as:

$$\text{Upstream Load} + \text{In River Erosion} - \text{In River Deposition} = \text{Net Transport Out}$$

The net transport out term can be positive or negative for upstream transport. Based on sources of sediment to the river, a qualitative diagram of the two conditions can be illustrated as in Figure 19. Low flow conditions create a low level of net sediment transport upstream and an even lower input from the river. During these conditions a net deposition balances out the net influx of sediments. During a high flow situation, the upstream loadings coming over Dundee Dam increase significantly and the net transport out of the LPR also increases significantly. Some unknown amount of greater erosion and deposition occurs in the river.

Combining the upstream river loading estimates developed by HQI for Dundee Dam and other tributaries with the sediment fluxes computed from the moorings from the three mooring deployments, a total cumulative sediment transport and net deposition of sediments in the river can be calculated. These calculations are approximations based on discrete datasets during varying time periods and have uncertainty associated with them; therefore, these calculations are meant to be more qualitative than quantitative.

Figure 20 shows flow rate and estimated cumulative transport out of the river near RMs 3 to 4.2 from October 1994 through January 2010. The bottom panel shows cumulative river input from Dundee Dam and tributaries and the estimated transport in the lower river near RMs 3 to 4.2. The figures show that during low flow periods the net input from upstream is negligible while the transport from the Bay into the river causes a net upstream transport. According to these estimates, the upstream transport occurs approximately 50% of the time. Periods where the dashed line is below the solid line in the bottom panel shows material trapped in the river during these time periods. The net sediment transport downstream, through the RM 3 to 4.2 reach during this time period is 41,000 MT/yr, or approximately 7% higher than the load coming in from upstream. The regular fluctuation throughout the time period of export vs. trapping of sediment in the LPR, leads to an interpretation of a system approaching equilibrium above the region of RMs 3 to 4.2 (i.e. no strong signal of net erosion or deposition). These values are based on a few discrete time periods of measurement and are for general illustration purposes only.

In order to help validate the conceptual understanding and the preliminary sediment transport model developed by HQI, the water column fluxes calculated in the model can be examined at various points in the river. Figure 21 shows the daily water column solids transport vs. flow rate at 8 stations in the LPR. The spatial summary shows that during low flow rates there is a significant upstream sediment transport (points on the lower half of each graph) in the river miles below the salt front (RM 9.8 and lower). Above RM 9.8, the magnitude of upstream transport reduces with the upstream stations. As the flow increases above 100 m^3/s (3530 cfs), the river shifts to strong downstream transport. The plots illustrate that during typical river flow, the strongest estuarine (i.e. upstream) net flux of sediment to the LPR occurs at the locations of the salt front and ETM.

MORPHOLOGY

To better understand the long- and short-term behavior of the sediments in the LPR, it is critical to examine the morphologic behavior of the river. The river has been significantly modified through dredging over the past century. Figure 22 shows the depth of the river channel based on a 2004 bathymetric survey as well as the original project depths (MPI, 2007). The original project depths were 3 m (10 ft) upstream of RM 8. Sediment accumulation of 4.8 m (15 ft) or more has occurred below RM 8 while changes have apparently been much less above RM 8. Since RM 8 is also the median extent of estuarine circulation, it is reasonable to conclude that the upstream transport of sediments has been effective at filling in the estuary.

BATHYMETRIC CHANGE

An illustration of the infilling of the LPR after cessation of dredging is shown in Figure 23. This figure shows approximate bathymetries of the LPR over time, derived from historical charts by Chant et al. (2009). Infilling after dredging ceased did not occur uniformly, but was focused at the upstream end of the dredged channel and worked its way downstream over time. This is consistent with geological understanding of the long term fate of drowned river valley estuaries in which sediment infill most rapidly near the limit of salt intrusion (the vicinity of the turbidity maximum). Chant et al. (2009) and MacCready (1999) have surmised that the deepening of channels due to dredging or other processes is accompanied by a more landward extent of estuarine circulation, which results in dispersion of sediments farther upstream. Thus, it is likely that the rate of deposition has varied spatially and temporally as the LPR is readjusting towards its equilibrium morphology.

Additional bathymetric analysis of surveys from 1989 to 2004 in the LPR provides evidence of the infilling trend over the recent term. Figure 24 shows the net bathymetric change calculated from statistical simulations using the survey data. The behavior shows expected morphologic behavior with some erosion on the outer bend where higher velocities are expected, yet the rest of the section shown is net depositional consistent with the overall infilling trend. Over the time period, the average infill rate was estimated to be 51,000 m^3/yr (66,700 yd^3/yr) (MPI, 2007). The surveys analyzed also showed that approximately 90% of the material has deposited within the lower 7 miles of the river. These long term observations are consistent with the overall sediment transport conceptual model. In the shorter term, year to year bathymetric surveys showed high variability in erosion and deposition patterns.

PILOT DREDGING BATHYMETRIC CHANGE

In December of 2005, a group of federal and state agencies, led by New Jersey Department of Transportation, conducted a pilot dredging project near RM 3. Approximately 4150 CY (3200 m^3) of contaminated sediment was removed. Figure 25 shows the pre-dredge and post-dredge surveys of the region, where the removal area is outlined by a white dashed line. For reference, all of the illuminated images in this report are illuminated with a sun angle of 315^o on the azimuth and 45^o on the elevation. Periodic surveys were done after dredging in order to monitor the status of the dredged area. The observations showed a rapid infilling of the dredged region. By 2008, no visible dredged areas remained. The channel experienced infilling until the sediment bed achieved the surrounding elevations.

The removal of approximately 4150 cubic yards of material from the river channel in 2005 changed the configuration of the river bed locally. The change results in lower currents in the vicinity of the dredged region. In turn the shear stresses near the sediment bed decrease as the square of the decrease in velocity. The net result is enhanced deposition of sediments passing through the area. As mentioned previously, sediments are continually transported tidally back and forth through this region of the river and can be seen in the water column monitoring data. When sediments pass a disturbed region of the bed with lower shear stresses, some portion of that sediment near the bed is deposited and trapped at the bed. Figure 26 shows the accumulation of sediment in the dredged region in subsequent surveys. Most notably, deposition of a foot or more occurred in some areas between surveys. Typically these are near the side walls of dredged region where the most dramatic change from ambient to disturbed bottom velocities occur. Table 2 presents the volumes of material infilling the dredged region between surveys.

Table2. Net change in sediment volume in the vicinity of the pilot dredging project.

From Date	To Date	Time Span (days)	Deposition (CY)	Erosion (CY)	Net Change (CY)
Consecutive Surveys					
11/28/2005	12/11/2005	13	2	**3828**	
12/11/2005	2/15/2006	66	1641	18	1623
2/15/2006	4/18/2006	62	829	7	822
4/18/2006	9/14/2007	514	1035	89	946
9/14/2007	11/28/2008	441	2	806	-804
Longer Time Intervals					
12/11/2005	4/18/2006	128	2453	3	2450
12/11/2005	11/28/2008	1083	2677	65	2613

The initial erosion volume of 3828 cubic yards, shown in Table 2, was calculated from the difference between pre- and post-dredging multibeam surveys, and is within 8 percent of the 4150 CY volume reported from the dredging operations. Values discussed subsequently to characterize the infilling are relative to the 4150 CY volume. Infilling is indicated by positive net changes, as shown in the four-month period following dredging, representing approximately 60% of the volume dredged. Infilling in the 17 months between April 2006 and September 2007 accounted for an additional 23% of the dredge volume, although most of that volume was subsequently eroded in following 15 months. There is no evidence in the multibeam dataset of preferential scouring of the dredged region suggesting that deposited sediment consolidates to ambient strength rapidly. The full net change in the final row is approximately 63% of the amount of material removed during dredging, suggesting that some additional infilling could be expected. The pilot dredging example shown here illustrates that if the river bed is perturbed over limited spatial areas, it rapidly moves back to the ambient conditions.

MORPHOLOGIC FEATURES

To better understand the finer scale features of sediment transport in the river, it is useful to define morphologic regions of the river. Using the 2008 high resolution multibeam survey data, eight different morphologic features were used to describe the commonly observed features in the LPR. The regions are:

1. Abutment – Hard structures such as bridge piers or scour protection in the vicinity of bridges that can alter flow and scour patterns.
2. Abutment Scour – Readily identifiable scour due to abutment features.
3. Broad Shoal –Broad mudflats and/or point bars typically located on the inside of river bends.
4. Island – In the upstream portions of the river, above water island features are present.
5. Margins – Broad channel margins near the shoreline that are often similar to the broad shoals but can also be anthropogenic shoreline features.
6. Smooth Channel – Broad relatively flat central channel present through much of the river. Although there are perturbations, the overall feature is considered smooth.
7. Deep Scoured Channel – Channel regions that typically occur on the outside of river bends where there is enhancement of velocity and shear stress, resulting in the maintenance of a deeper scoured feature at these locations. The delineation is not meant to suggest that these are long term net scour features.

These qualitative morphologic definitions are intended to help understand the general lateral and longitudinal features in the river. Identification of these features can help to better understand transport trends and more effectively design remediation. Figure 27 through Figure 29 illustrate the multibeam survey data and the identified morphologic regions of the river in the vicinity of RM 2, RM 4, and RM 6. The point bar deposition/ mudflat regions on the inside bends, where the current velocity is lower, fall in line with what one expects in typical curving channel flow. This behavior can be observed nearly uniformly throughout the river with corresponding deep channels on the outer bends where the current

velocity is higher. The presence of these features suggest that during high river flow events, the highest shear stresses and higher probability for erosion can be expected in the deeper channels and the lowest shear stresses and higher probability for deposition can be expected on the shoals. Additionally, the long-term presence of the features shows that the tidal currents maintain the channel morphology, such as the presence of deeper channels, during periods of net sediment influx from the direction of Newark Bay.

Both typical and atypical bedforms exist in the channels of the LPR. Figure 30 illustrates bed features near RM 3 and RM 8. Near RM 3, where the sediment bed is predominantly fine material, typical sand waves and ripples do not form; although, there are perturbation features (i.e. lumps) at the river bed (possibly large detritus mounds or clumps of stiff material of unknown origin) that show a shallower slope on the upstream lee of the feature. This feature suggests a net upstream direction to near-bed sediment transport at the time of the survey. The RM 8 bedforms are typical of uniform sand waves moving downstream with the smooth slope facing upstream. The shape of the feature has a dominant downstream directionality. The bedforms suggest that the bidirectional flow in this region was not significantly affecting the bed in this region at the time of the survey (low flow).

SEDIMENT BED

Looking at and into the sediment bed can provide information on the long- and short-term behavior of sediments in various regions of the river. One of the most basic sediment bed properties is the particle size. In addition to a large number of surface grabs of approximately 15 cm deep that were collected as part of the 2005 field effort, a side scan survey was conducted. The particle size measurements were used to calibrate a bottom textural classification based on the side scan reflectivity. The data provide a broad delineation of surface rock, gravel, sand, and silt. The data are limited in that they often do not distinguish between more detailed classifications such as sandy silt or silty sand, and represent only the surface of the sediment and not the 15 cm sample depth of the grab. Figure 31 shows an overlay of the bottom type on the river. The lower eight miles of the river are dominated by silt material with pockets of silt and sand. River mile 8 shows a dramatic shift to sand and gravel sediment with pockets of silt. Figure 32 shows a close up of this fairly sharp transition. Although the side scan data provide a continuous delineation, it is based on surface conditions which can vary rapidly with flow. Some level of variation can be expected. The transition at RM 8 is again associated with the extent of the salt front and estuarine circulation propagation which delivers and traps fine sediments at the bed. The reasons for the coarser sediment size upstream of RM 8 are likely a combination of winnowing due to high river flows and the proximity of bedrock and potential sand and gravel sources to the bed of the river in the upstream regions.

The 2005 grab samples and the 2008 CPG low resolution core data can be combined to develop a more comprehensive picture of the surface sediment. The data were used to calculate percent fines at each core location (material less than 63 micron size). These values were interpolated over the river bed and are shown in Figure 33. Although the side scan interpretation identified many of these areas as silt, they may be sandy silt or silty sand in a more detailed classification. Both the original surface grabs from 2005 and the 2008 cores show that there are silty sand regions in the lower river, yet these sediments are still generally classified as fine dominant.

The particle sizes correlate strongly to morphologic regions in the river. The highest fine content is located on lower energy inner bends of the river identified as broad shoals in the morphology maps. The higher velocity channel regions and deeper scoured channels generally have higher sand content. The strong correlation suggest that using morphology to guide the distribution of sediment properties in modeling work can be investigated to provide an accurate method to extrapolate limited datasets.

Radioisotope data has also been utilized to provide a geochronology of the river sediment in specific locations. Cesium-137 (Cs-137) profiles in cores collected as part of the 2005 CSM sampling provide a good picture of historic deposition trends in the lower river. The 2005 cores were collected at five locations in the river which are shown in Figure 34 and Figure 35. The peak of Cs-137 activity is referenced as the peak of atmospheric nuclear testing in 1963 (Figure 36). The broadest shoal/point bar at RM 2.2 has the deepest peak of Cs-137 suggesting the highest deposition rate. All of the peaks are below 1 m (3.3 ft) with the exception of the core at RM 7.8 which is adjacent to a scour depression near a bridge abutment. The trend in these cores provide another line of evidence suggesting that the long term river behavior is consistent with our conceptual model of infilling in these areas.

An additional data source which provides information on the river sediments is the 2005 SPI camera survey. The purpose of the SPI survey was to characterize the physical and biological condition of surface sediments and assess the river's intertidal and subtidal benthic habitats by using a camera prism that slices into the sediments providing an in-situ view of the sediment. Prior to June 2005 a large flow event appears to be responsible for delivering a large magnitude of sediment to the river. The SPI camera can be used to identify the most recently deposited sediment horizon at different locations. Figure 37 shows images and points of the SPI camera transect at RM 3.9. The inside bend of the river had the highest recent deposition of 12.6 cm (4.96 in) where the deposited material is composed of macro-organic leaf and stick detritus. The deep channel of the river had a low recent deposition of 1.9 cm (0.74 in) and shows a much more uniform sediment column of anoxic material below a surficial oxidized layer. A review of all SPI camera data not only supports the observation of cross-channel gradients in transport and morphology (e.g. gradients in deposition and sediment layering), but also shows that detritus plays a potentially significant role in transport in the river. It is important to note that the SPI camera, particle size, and textural data provide only a temporal snapshot that is dependent on the river flow conditions in the months preceding the collection of each data set; therefore, there is expected to be temporal variation in the specific trends noted here.

Sediment erosion rate data generally provides an important indicator of down core sediment transport potential at coring locations. Sedflume is one common device for quantitatively characterizing sediment erosion rates. Sediment cores were collected from 14 sites along the Passaic River and analyzed in the USACE Sedflume mobile laboratory. Two cores were collected as replicates at each location for a total of 28 cores. The results of the bulk property analysis and erosion rate experiments have been presented and discussed in the report "Erodibility Study of Passaic River Sediments Using USACE Sedflume" (Borrowman et al., 2006).

Figure 38 shows the sites along the river where the cores were collected. Sediment cores from sites P01 through P12 were generally silty, while cores from P13 through P16 were sandy. Replicate coring at each of the 16 sites varied in separation from about 1 to 10 m. A non-dimensional erosion rate ratio calculated by comparing an individual core's erosion rates to site wide averages for the top 5 cm over a range of

shear stresses is useful for qualitatively comparing the erosion rate data. Figure 39 shows the erosion rate ratio for the silty cores on the LPR. Replicate sites, shown as adjacent columns for each core location in the figure, were within 10 m of each other and show widely varying erosion rate ratios. At many specific locations, varying sediment properties and erosion rates were observed with depth. Additionally, the columns are colored by qualitatively identified morphologic region. No clear correlation is seen as a function of morphologic region. Analysis of these cores has indicated that the fine sediment erosion properties in the river are heterogeneous over small spatial scales, yet the erosion rate data do provide general sediment behavior for use in modeling studies.

NEWARK BAY

Sommerfield and Chant (2010) conducted extensive moored measurements of hydrodynamics and sediment transport and sediment characteristics from 2007 to 2009 in Newark Bay. Since the sediment transport in the LPR is so closely linked to Newark Bay, it is important to understand the general trends in Newark Bay. The key result of the study was that approximately 86% of sediment transported into Newark Bay during the study is from Kill Van Kull in the south eastern portion of the bay. The LPR by contrast contributed 10% of the measured sediment transport. Sommerfield and Chant (2010) postulate that the net sediment flux from Kill Van Kull has increased substantially due to deepening of Newark Bay due to dredging.

MARCH 2010 HIGH FLOW EVENT

On March 16, 2010, a peak flow at Little Falls of almost 450 m^3/sec (15,800 cfs) occurred. This is in excess of a once-in-25 year event. The event provided a unique opportunity for the collection of water column and multi-beam bathymetric data to assess the effects of a large event on the river. R. Chant (Rutgers) conducted measurements of TSS using grab samples and a calibrated optical backscatter meter down the centerline of the lower 8 miles of the river. Figure 40 shows preliminary TSS along a longitudinal transect from the cruise. The section shown was measured during an ebb tide when the downstream transport is expected to be at a maximum. The figure shows the ETM moved out to approximately RM 1 with a peak concentration in excess of 400 mg/L. The position is consistent with the Chant et al. (2009) measurements of ETM position during a 330 m^3/sec (11,665 cfs) flow rate. The net effect is to transport sediments farther down river and out to Newark Bay.

A multibeam survey was conducted mid-June 2010 approximately 3 months after the high flow event. Comparison of features in the river allows for some observations of river behavior during high flow events. These comparisons are qualitative in nature and no attempt is made to quantitatively compare bathymetric change. Figure 41shows the region in the vicinity of the pilot dredging area. Most notably, the deposition over the intervening years since the dredging has remained relatively stable with no large scour features evident. In the northern edge of the channel a linear scour depression has experienced infilling and the sediment bed is now relatively featureless. Small perturbations in the deeper channel have remained in place and some possible exposure due to scour is seen on the eastern side of the dredge footprint. Figure 42 shows a comparison of a channel region near RM 3.5. Morphologic evidence of scouring can be seen around hard features with smaller channels developing. This comparison suggests some scour in the deeper channel, but the broader flats on the inside bend show little morphologic change. Figure 43 shows the appearance of bedforms near RM 9.8. Note that this is a different location than the bedforms observed in Figure 30. These bedforms were not present in either the 2007 or 2008 multibeam

surveys, suggesting the formation and downstream movement of sandy bedforms during higher flow events.

SUMMARY

A conceptual model of the interplay of estuarine circulation and river flow has been developed here. The importance of both of these processes on sediment transport during high and low flow conditions has been discussed and illustrated. Field and modeling data can be used to support the conceptual model of transport in the system and provide some quantification of these processes and their relative importance. Additionally, morphologic and sediment bed data can be used to construct a more detailed spatial and temporal picture of what is occurring in the river. Figure 44 and Figure 45 summarize the key qualitative concepts during low flow conditions dominated by estuarine circulation and upstream sediment transport and high flow conditions where downstream river flow dominates.

Generally the conceptual transport model can be characterized by the following points:

- The LPR typically has tidal delivery of sediment from the direction of Newark Bay into the LPR during low flow conditions due to estuarine circulation
  - The delivery of sediment is generally limited to the lower 8 miles
  - Tidal mixing due to erosion and deposition of the surface sediment (on the order of mm [Sanford, 1992])
  - The highest shear stresses in the deep channels maintain the channels while lower shear stresses on the shoals/mudflats maintain those features. These morphologic features have been present and persistent since at least the 1980's.
  - Based on analysis of the available water column data the upstream transport of sediment occurs at flows greater than the median flow, suggesting that upstream transport occurs a majority of the time. Although the transport direction may be upstream most of the time, the data show that the cumulative upstream transport of sediment is lower than the cumulative downstream transport during high flow events.
  - The area dredged during the pilot dredging project rapidly experienced rapid infilling in the subsequent four month period. Net erosion was noted over the following 2.5 year period.
- During elevated flow conditions, the river flow in the LPR dominates and there is a net flux of sediments out of the river to Newark Bay
  - During elevated river flows some portion of the unconsolidated sediment delivered from the Bay during tidal action and river during low flow is resuspended and transported into the lower miles of the LPR and the bay
  - Thick mats of organic detritus and gas generation, as observed in the SPI camera data, play a definite, yet un-quantified, role in sediment bed elevation and erosion property changes in the LPR

- The net downstream sediment flux during high flow events is orders of magnitude larger than daily upstream tidal delivery of sediment from the Bay

- The net sediment flux measured by Sommerfield and Chant (2010) was into Newark Bay over the long term and accounted for approximately 10% of the sediment entering the Bay during that time period

- The cumulative sediment export from the LPR from 1994 to 2010, based on preliminary estimates of transport, was approximately 7% greater than the material coming into the river from upstream sources (e.g. Dundee Dam). The value oscillates between net export and import over the time period as flow rate varies. Given the uncertainties involved in the estimate, it is likely that this is not significantly different from no net import or export. The results suggest that the LPR above RMs 3 to 4.2 is approaching equilibrium.

- The pilot dredging region showed bed responses to large events similar to the surrounding channel sediment suggesting that deposited sediment consolidates rapidly to ambient conditions

- Multibeam surveys conducted within 3 months of the March 2010 high flow event suggest some localized scouring in deep channel regions and deposition in shallower shoals may have resulted from the event. Importantly, hard features and perturbations in the deep river channel were unmoved during the large event suggesting little change in the river channel during high flow events.

- Long term transport has resulted in net deposition in the river over recent decades which appears to be slowing as the system approaches equilibrium

  - Dredging in the 1940's disrupted the preferred equilibrium of the system and has resulted in strong infilling of sediment since the cessation of dredging

  - Based on infilling rates over time from USACE and other surveys, the deposition rates in the lower miles of the river have decreased over time as the system approaches a quasi-equilibrium. The observations are physically consistent with the conceptual model of reduced channel size decreasing overall deposition potential.

  - Large events provide energy for erosion of the sediments. The potential for erosion is dependent on location in the river, strength of the event, and properties of the sediments.

  - More recent sediment deposits will generally be more mobile

REFERENCES

Borrowman, T.D., Ernest R. Smith, Joseph Z. Gailani, and Larry Caviness et al., 2006. Erodibility Study Of Passaic River Sediments Using USACE Sedflume. US Army Engineer Research and Development Center, Vicksburg, MS. June 2006.

Chant, R., Fugate, D., and Garvey, E. (2009). "The shaping of an estuarine superfund site: roles of evolving dynamics and geomorphology". Submitted for publication in Estuaries.

Dyer, K. R. 1997. Estuaries: A Physical Introduction. 2nd ed. John Wiley & Sons, Chichester, England.

Geyer, W. R., J. H. Trowbridge and M. M. Bowen (2000). "The dynamics of a partially mixed estuary." Journal of Physical Oceanography 30: 2035-2048.

HydroQual, Inc. (HQI) (2008). "Lower Passaic River Restoration Project and Newark Bay Study – Final hydrodynamic modeling report." US Environmental Protection Agency – Region 2. Us Army Corps of Engineers Contract No. DACW-02-D-0003.

Malcolm Pirnie, Inc. (MPI) (2007). "Draft Source Control Early Action Focused Feasibility Study." For U.S. Environmental Protection Agency, Region 2 under U.S. Army Corps of Engineers Contract No. W912DQ-06-D-0006.

MacCready, P. (1999). "Estuarine Adjustment to Changes in River Flow and Tidal Mixing." Journal of Physical Oceanography 12:708-726.

Ocean Surveys, Inc. (OSI) (2009). "Oceanographic in-situ and real-time data acquisition program, Passaic River, Newark, NJ". OSI Report No. 09ES045. Prepared for Tierra Solutions, Inc.

Sanford, L. P. (1992). "New Sedimentation, resuspension, and burial." Limnology and Oceanography 37(6): 1164-1178.

Sommerfield, C. and Chant, R. (2010). " Mechanisms of Trapping and Accumulation in Newark Bay, New Jersey: An Engineered Estuarine Basin (HRF 008/07A)". Report to the Hudson River Foundation, HRF Project 008/07A.

FIGURES

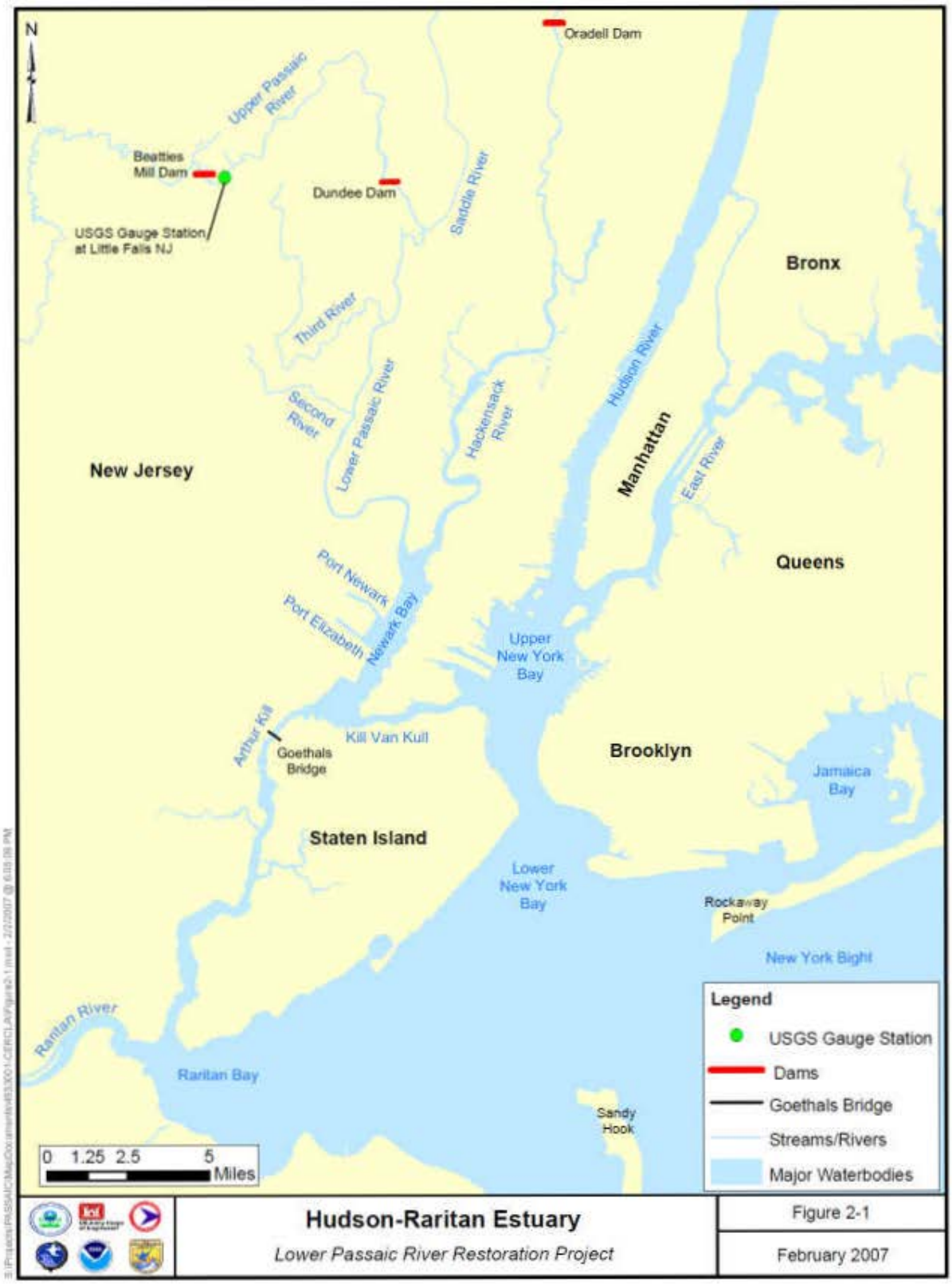

Figure 1. Map of the Lower Passaic River region (MPI, 2007).

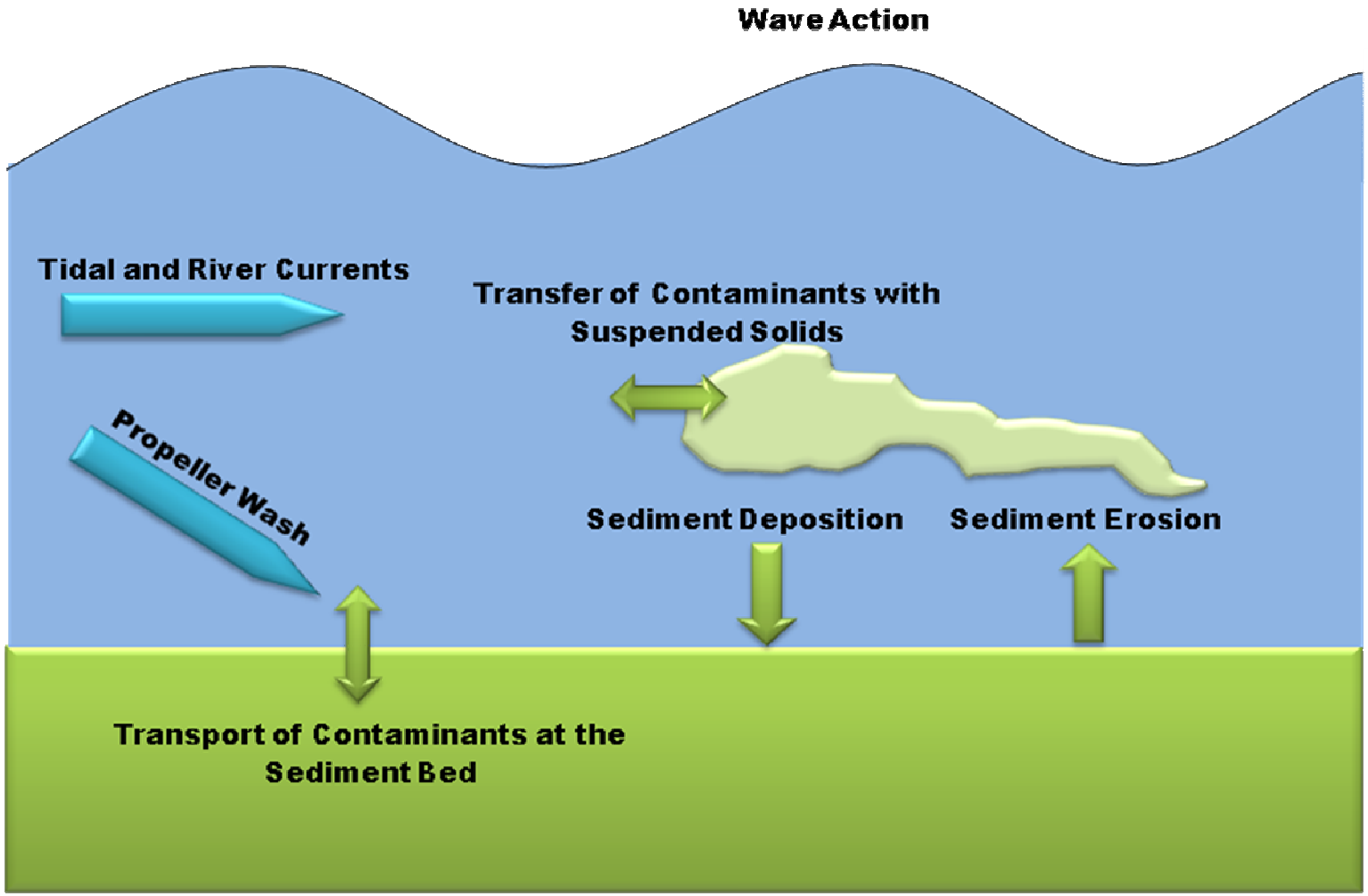

Figure 2. Conceptual diagram of processes related to sediment and contaminant transport.

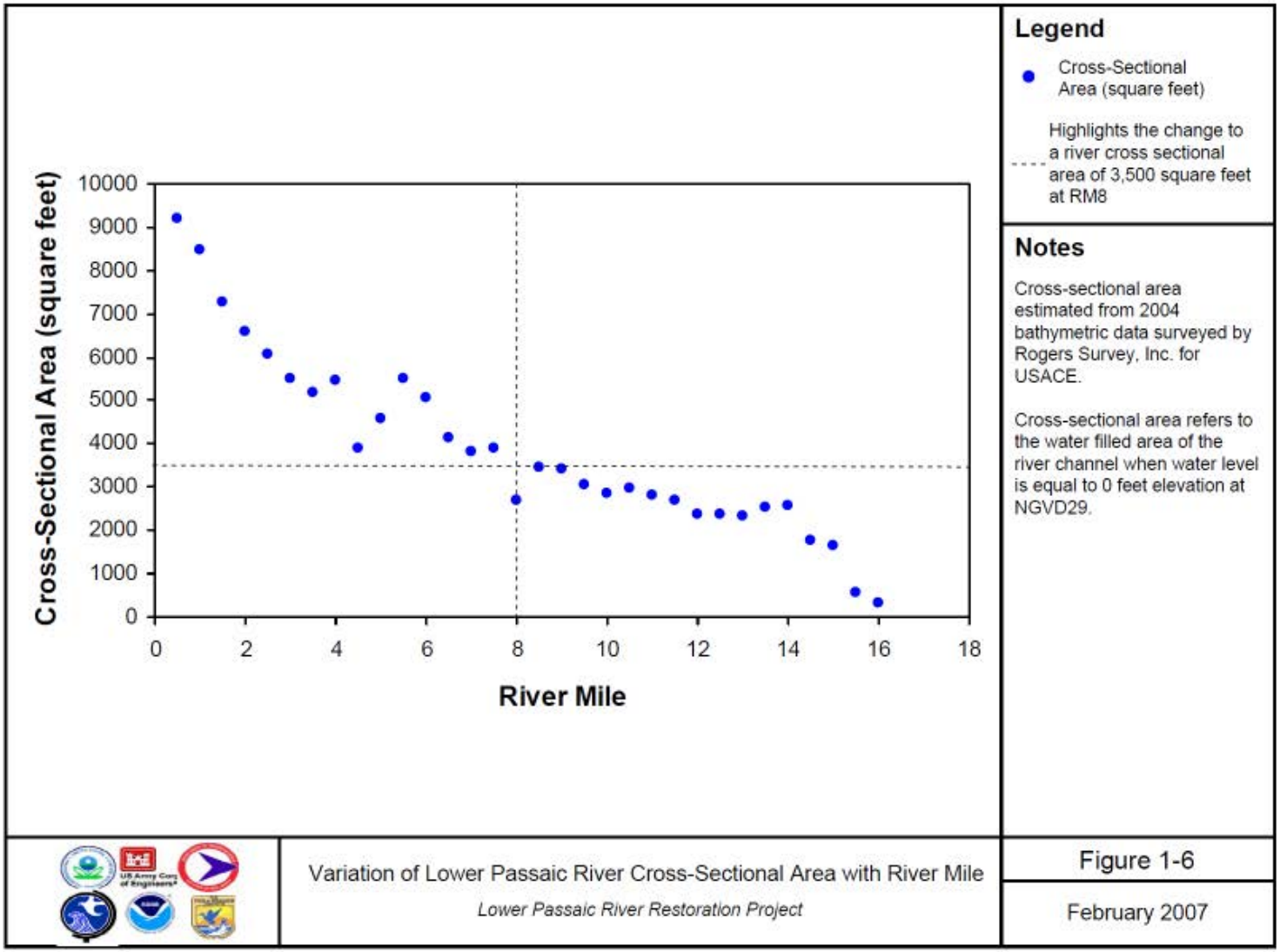

Figure 3. Variation in river cross-sectional area with river mile numbered from river mile 0 at the mouth (MPI, 2007).

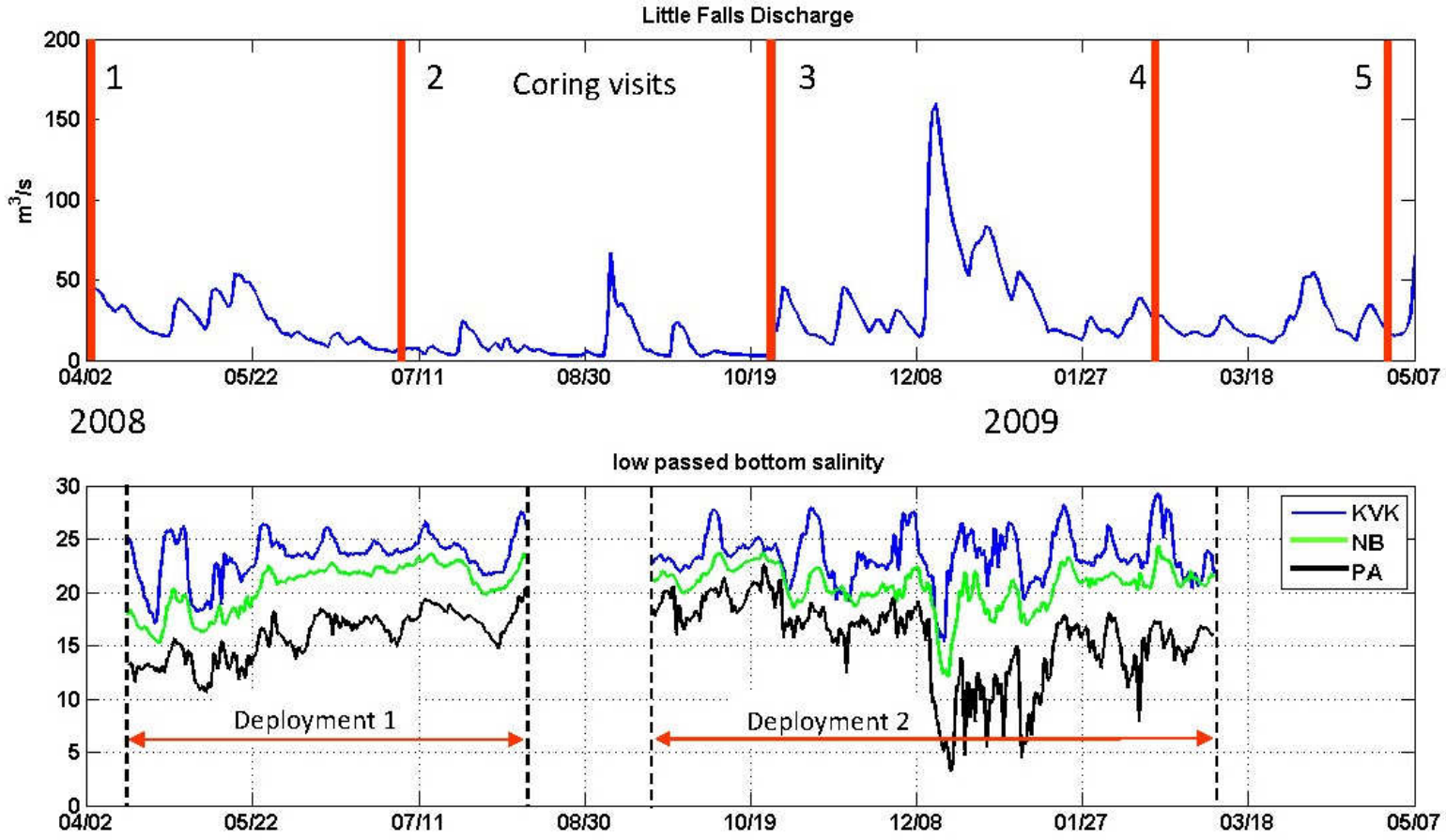

Figure 4. Timeline showing the times of coring (top) and mooring deployments (bottom) from the Sommerfield and Chant study (2010). Passaic River discharge at Little Falls and salinity data in psu are shown for reference. KBK=Kill Van Kull mooring, NB=Newark Bay.

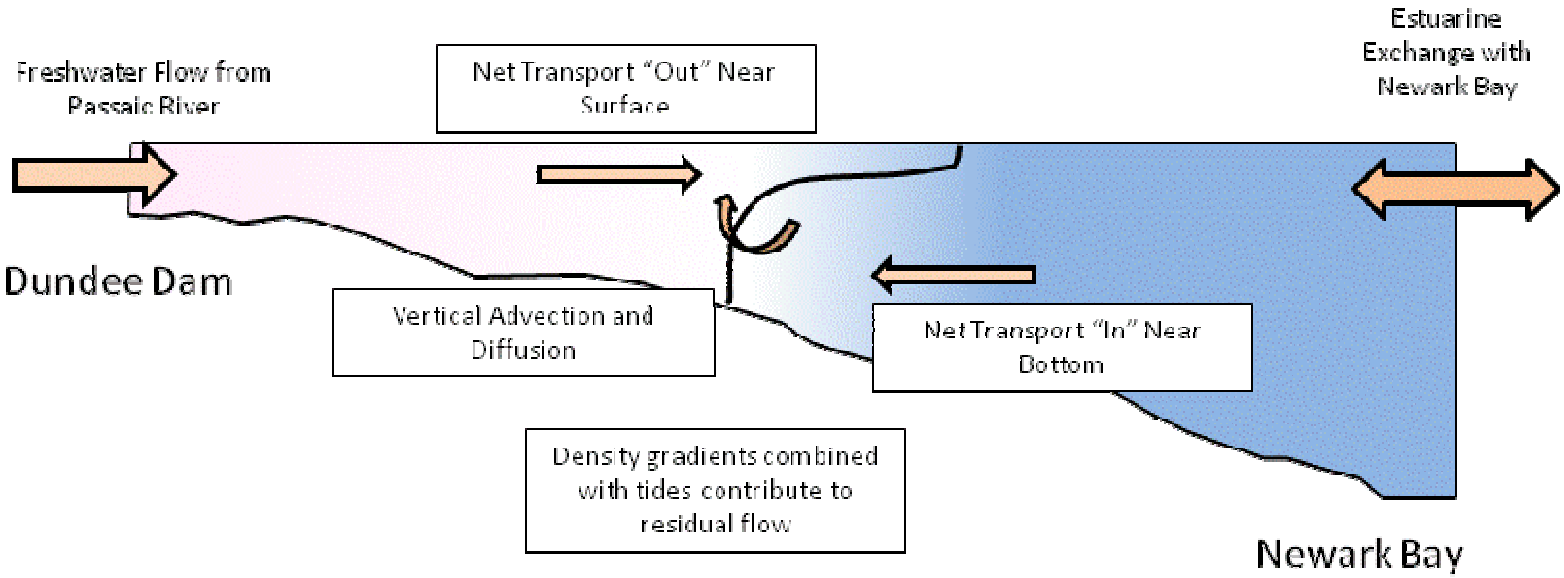

Figure 5. Estuarine processes active in the Lower Passaic River, a partially mixed estuary.

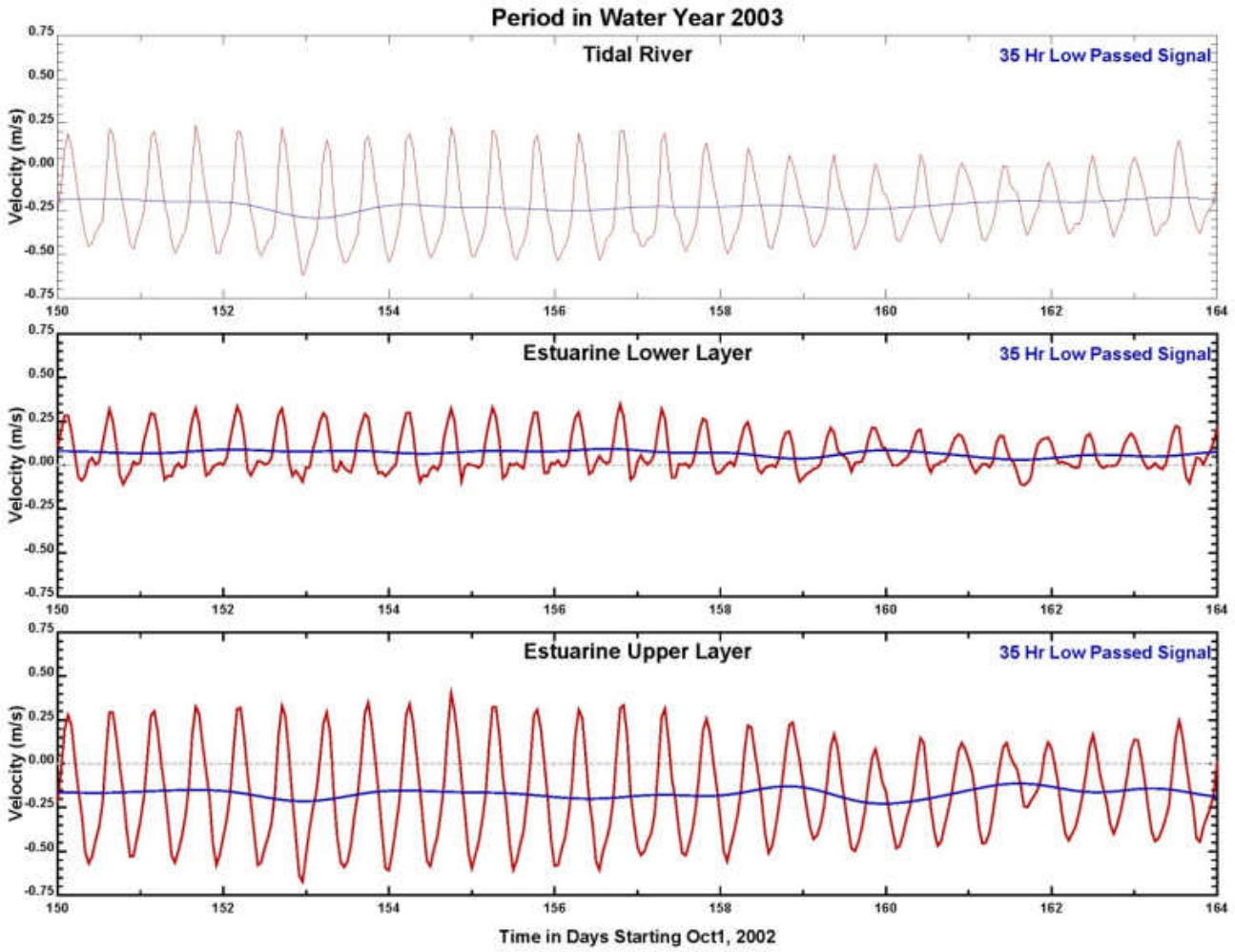

Figure 6. Time series of combined tidal (red) and tidally filtered velocities (blue) from the LPR hydrodynamic model (HQI, 2008), in the tidal fresh region (upper panel) and the estuarine region (lower two panels). Positive velocities are in the flood direction (upstream) and negative velocities are in the ebb direction (downstream).

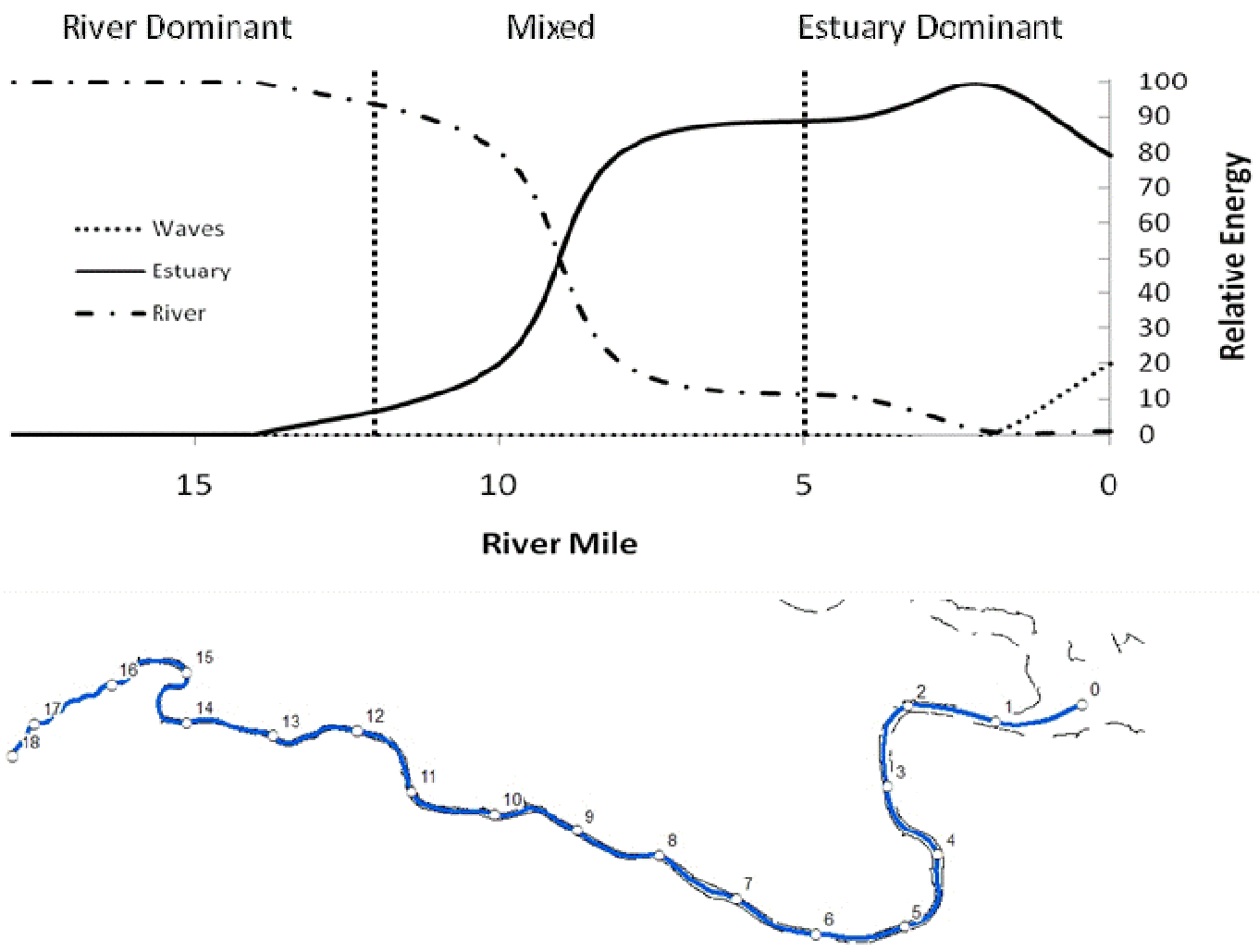

Figure 7. Conceptual contribution of three forcing factors relevant to transport in the Lower Passaic River. The figure represents median flow conditions at Dundee Dam.

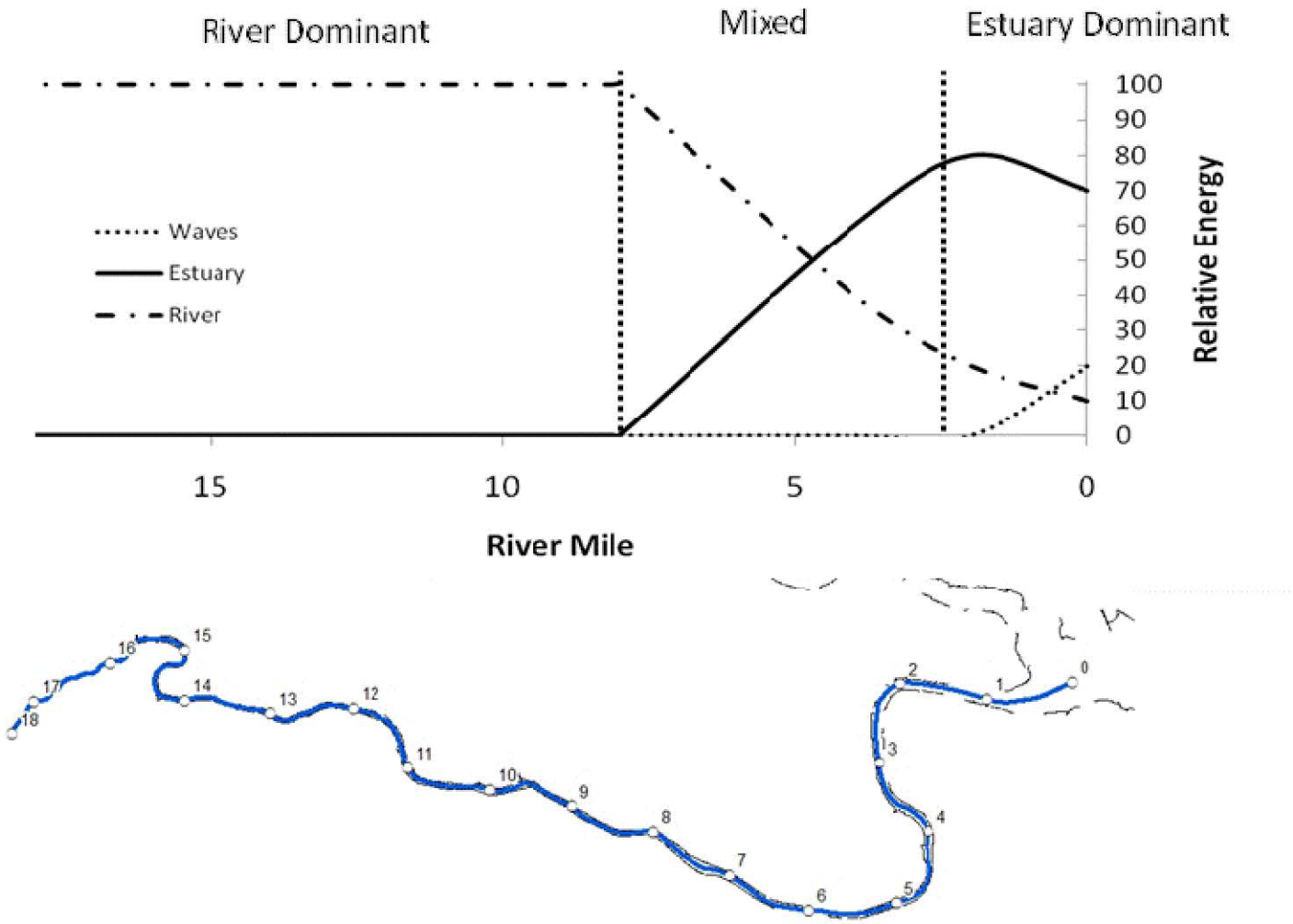

Figure 8. Conceptual contribution of three forcing factors relevant to transport in the Lower Passaic River. The figure represents elevated flow conditions at Dundee Dam.

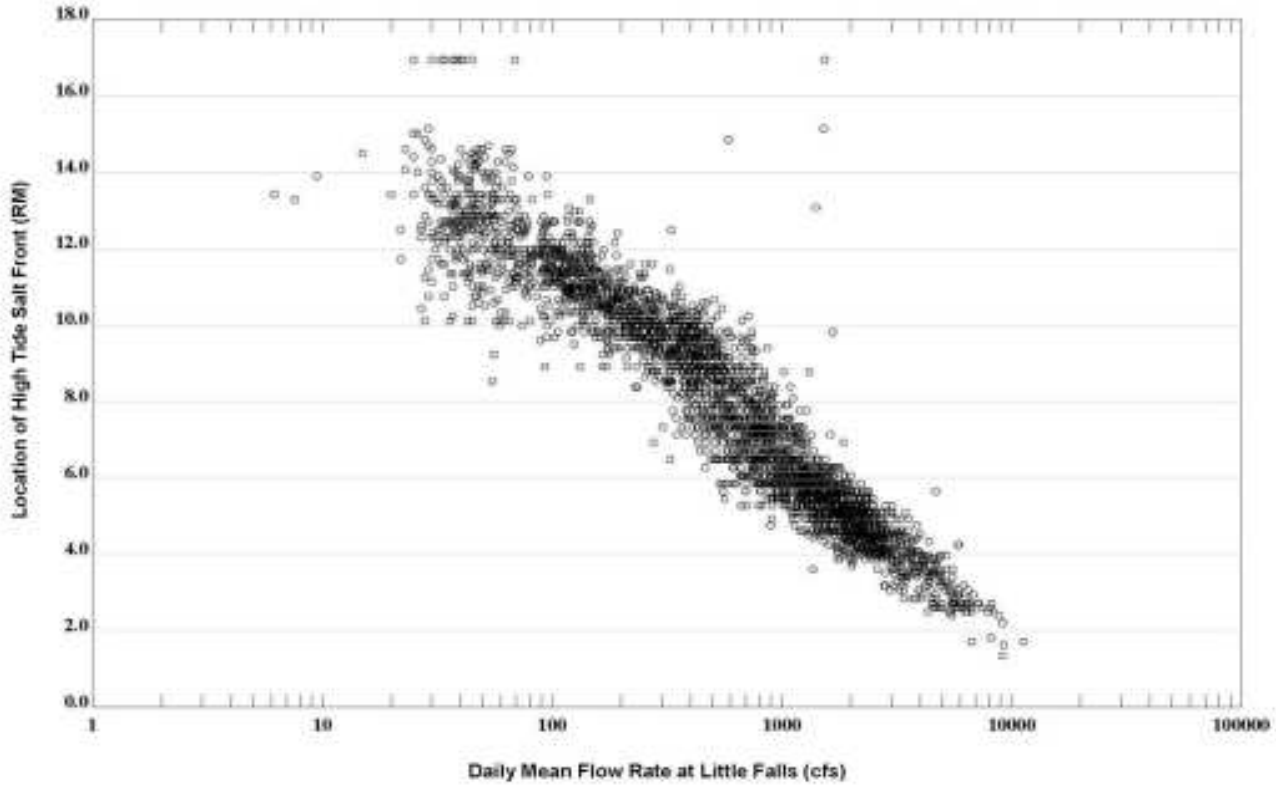

Figure 9. Location of high tide salt front as a function of flow rate determined from the HQI hydrodynamic model

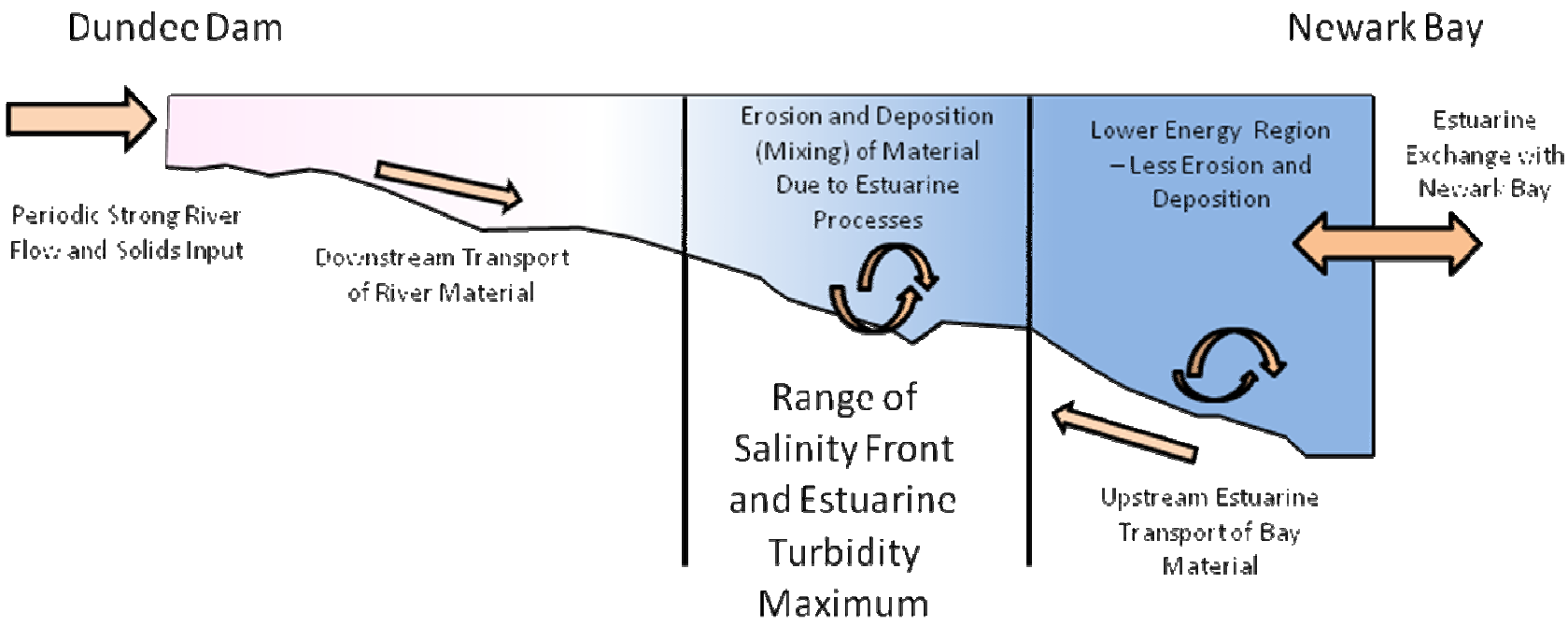

Figure 10. Estuarine and sediment transport processes active in the Lower Passaic River.

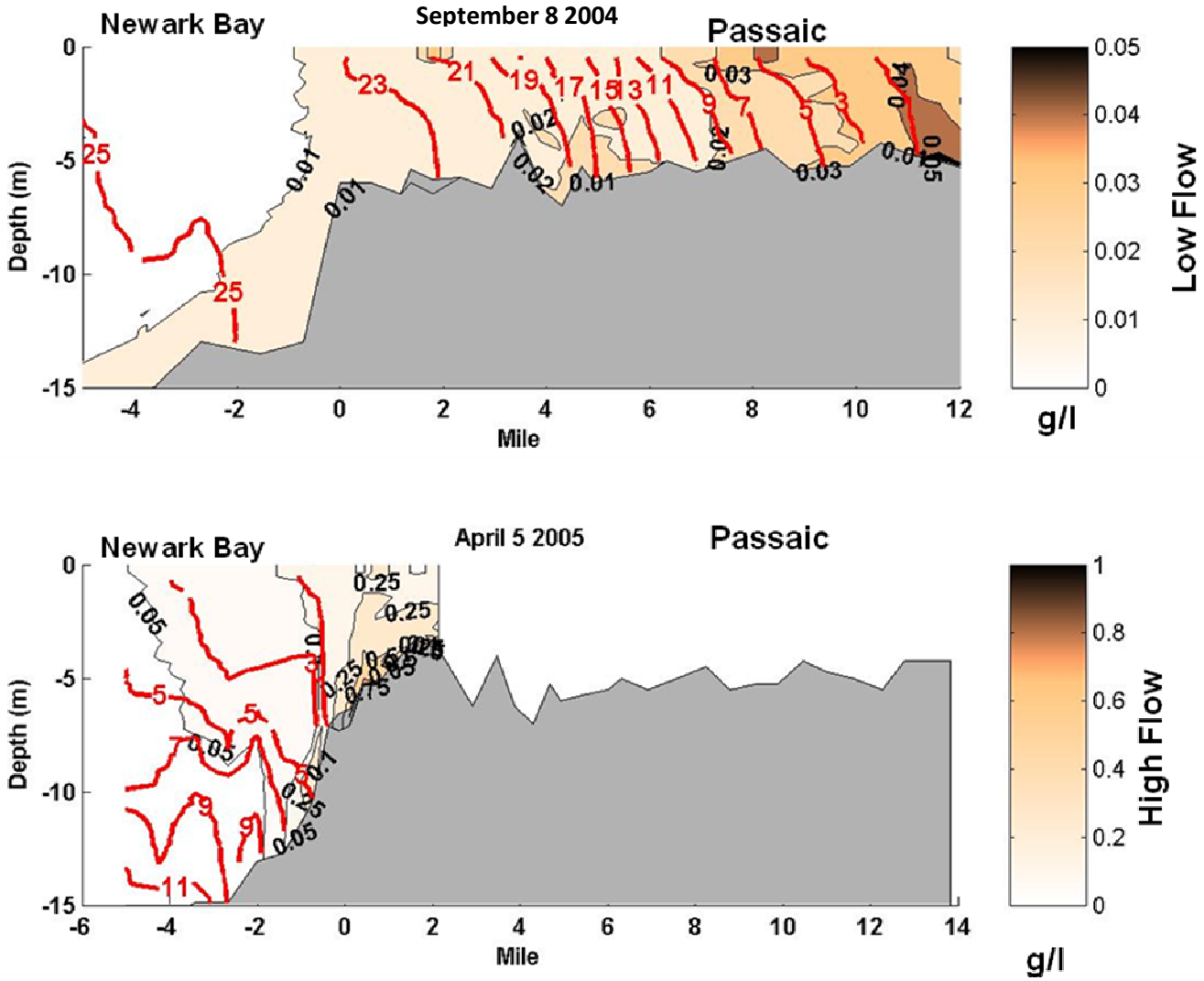

Figure 11. Longitudinal profiles of salinity and TSS from Chant (2009) corresponding to 1 and 330 m^3/s river flow rates respectively.

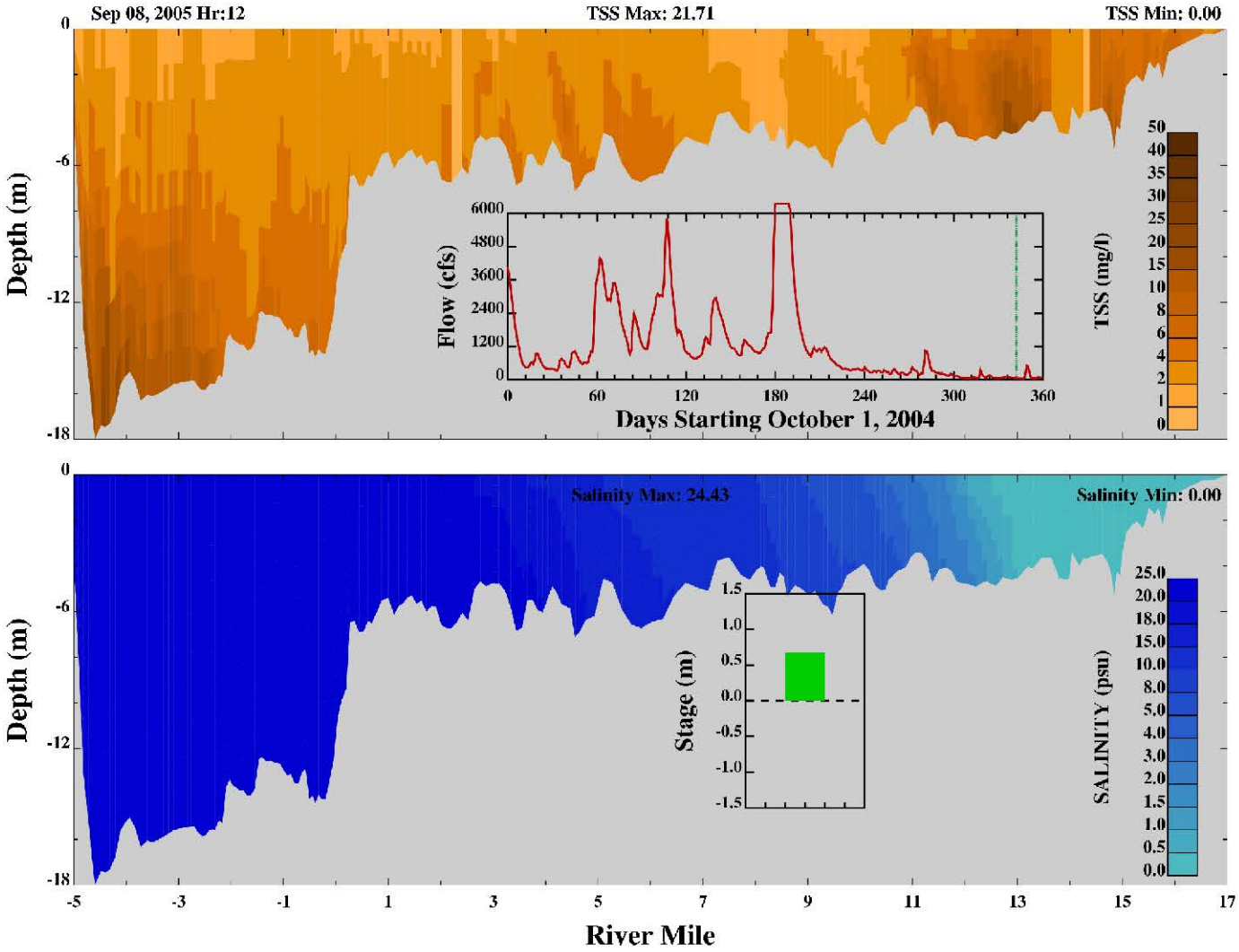

Figure 12. Longitudinal profiles of TSS (top) and salinity (bottom) during low flow conditions in September 8th, 2004 from preliminary HQI hydrodynamic and sediment transport model.

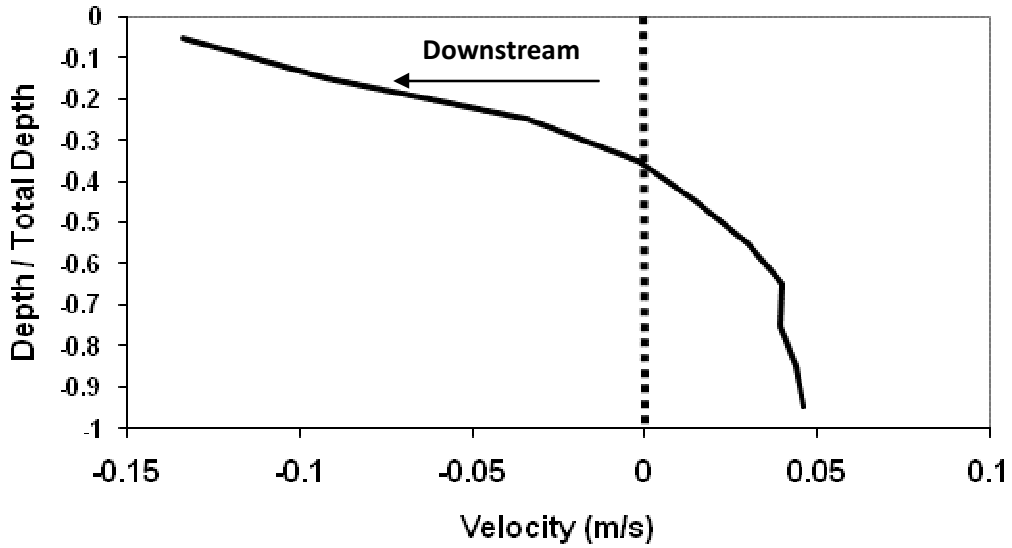

Figure 13. Tidally averaged velocity profile during low flow conditions in August 2004 from preliminary HQI hydrodynamic and sediment transport model. The profile is located at river mile 5. Negative velocity is directed downstream.

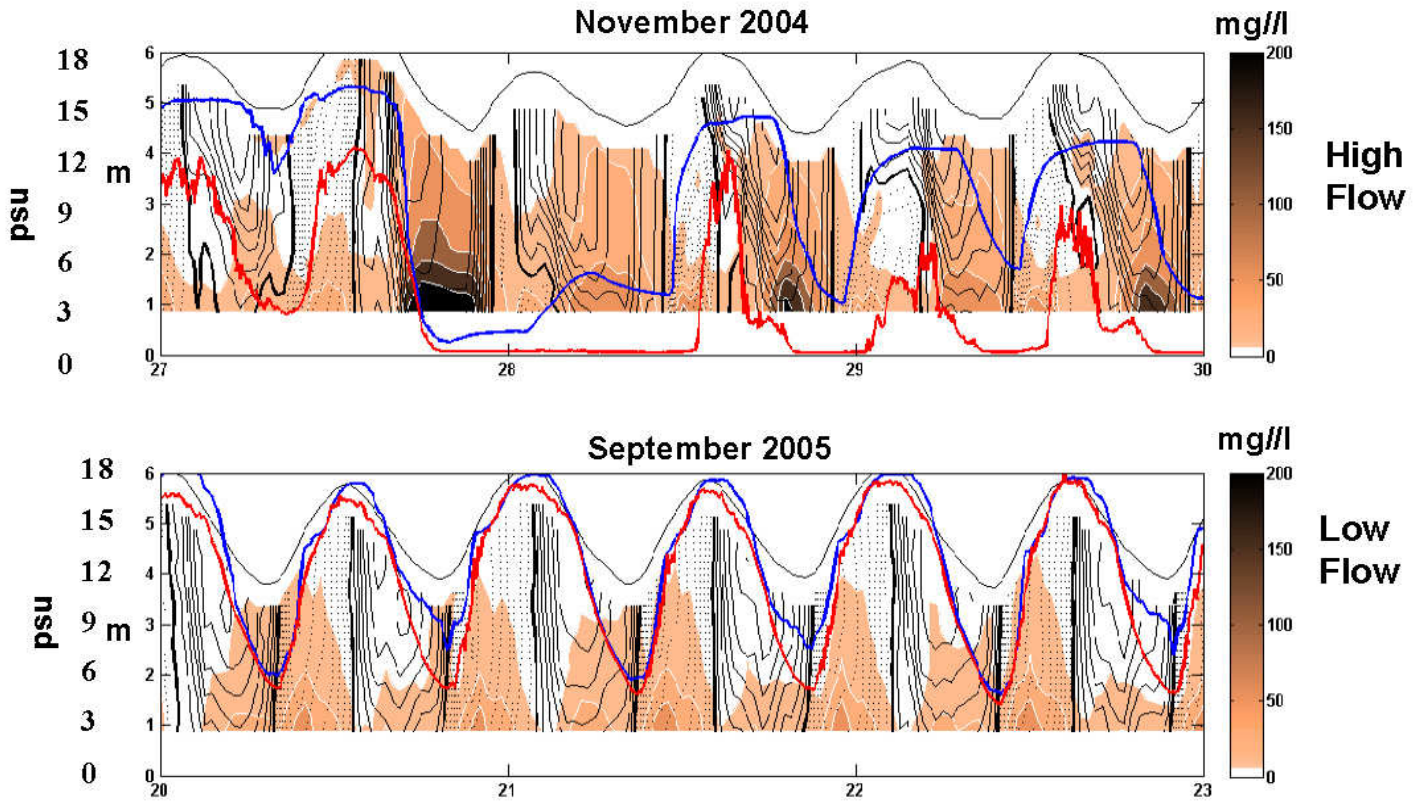

Figure 14. Time series profiles of salinity (red lines are surface and blue lines are bottom of the water column) and TSS (solid contours) near RM 3 from Chant et al. (2009) corresponding to high and low river flow rates, respectively.

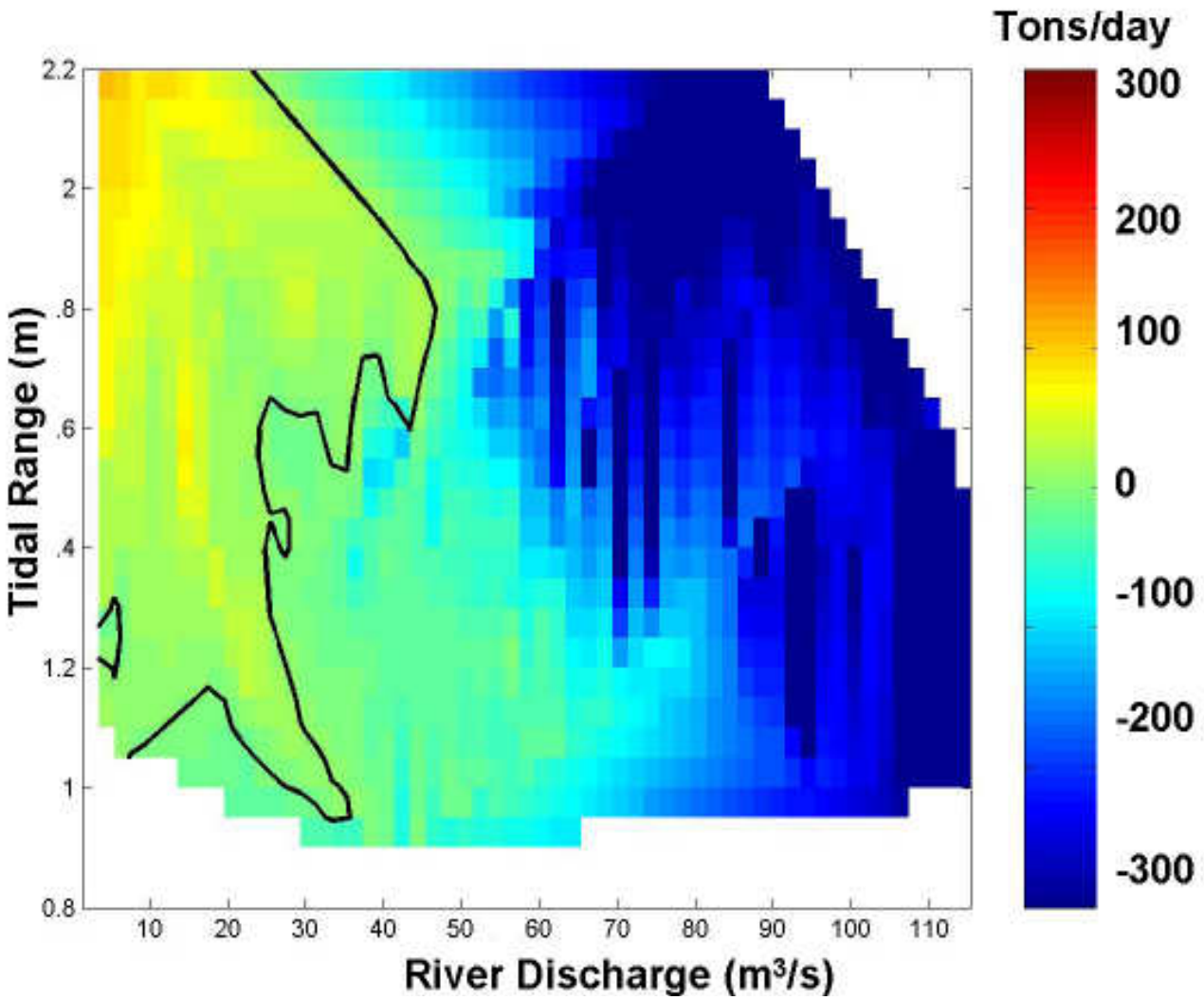

Figure 15. Sediment transport (positive is upstream) as a function of tidal range and river discharge (flow rate) estimated from current meter and backscatter measurements near RM 3 (Chant et al., 2009).

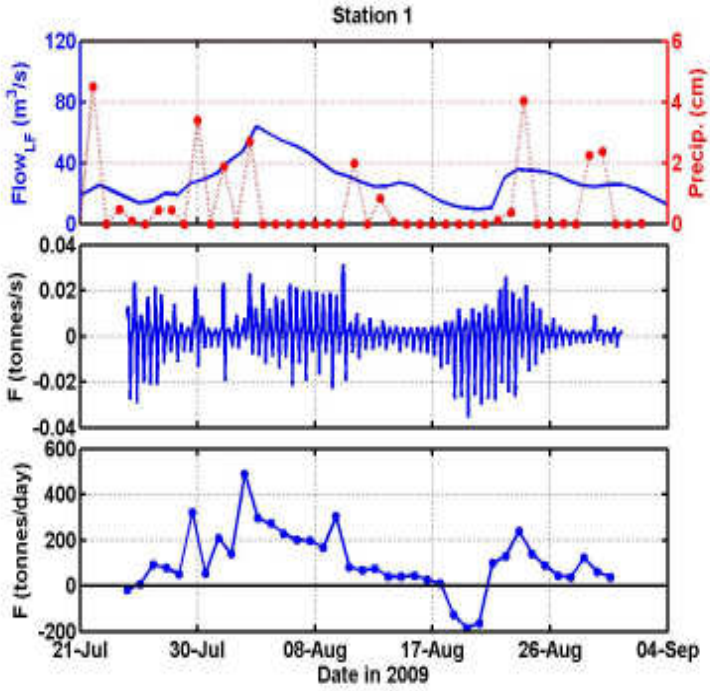

Figure 16. LPR flow rate and local precipitation during the summer 2009 instrument deployment (top panel). The instantaneous and daily averaged sediment fluxes are calculated for Station 1 (bottom panels).

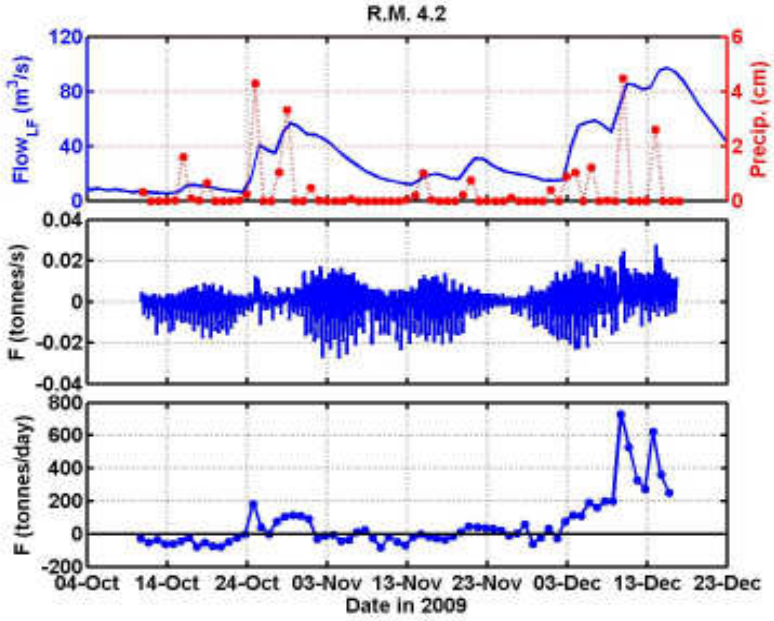

Figure 17. LPR flow rate and local precipitation during the fall 2009 instrument deployment (top panel). The instantaneous and daily averaged sediment fluxes are calculated for the RM 4.2 mooring (bottom panels).

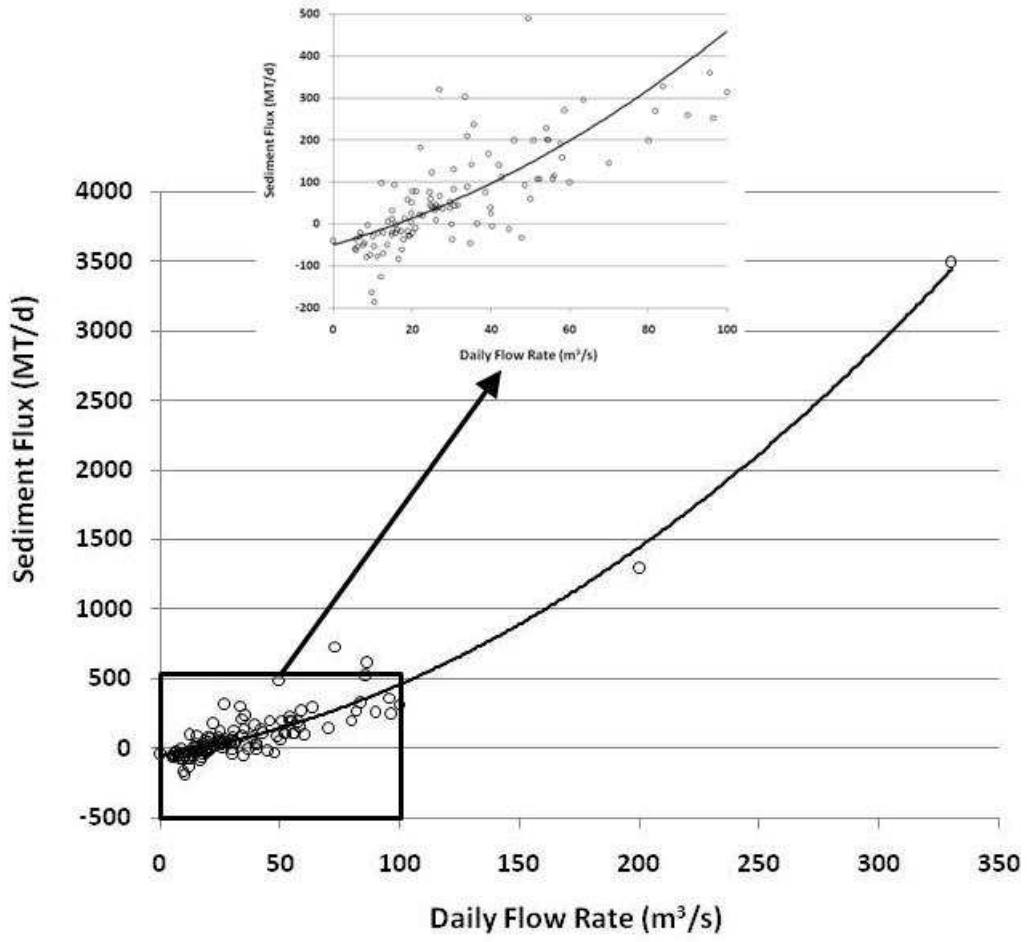

Figure 18. Daily averaged sediment flux as a function of river flow rate. The data is a combination of the stations between RM 3 and 4.2 from the Chant et al. (2009), Summer 2009 (OSI, 2009), and CPG Fall 2009 PWCM datasets and the data fit.

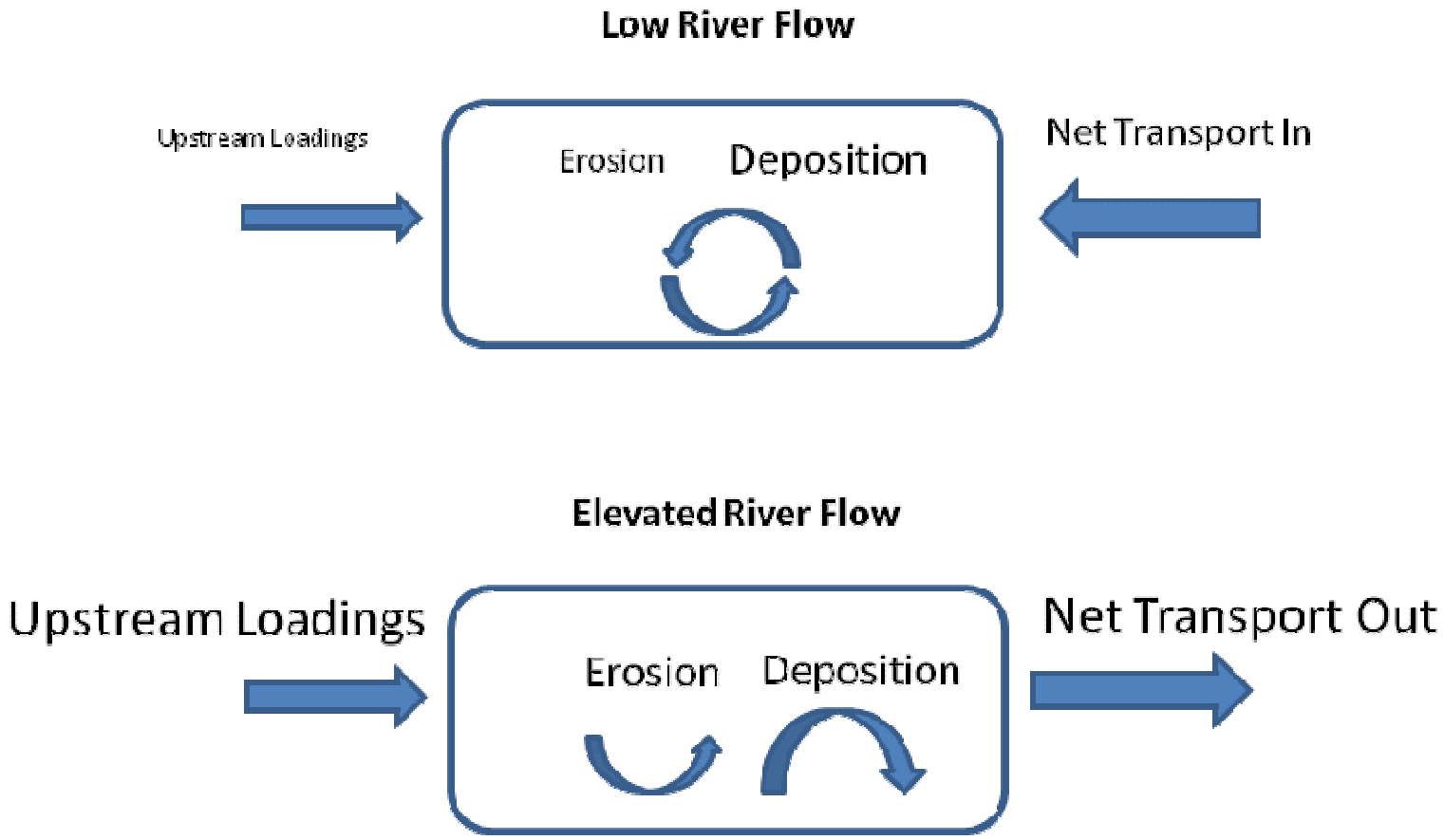

Figure 19. Sediment balance during low and elevated river flow periods. The size of each component is relative to the contribution of each term in the balance.

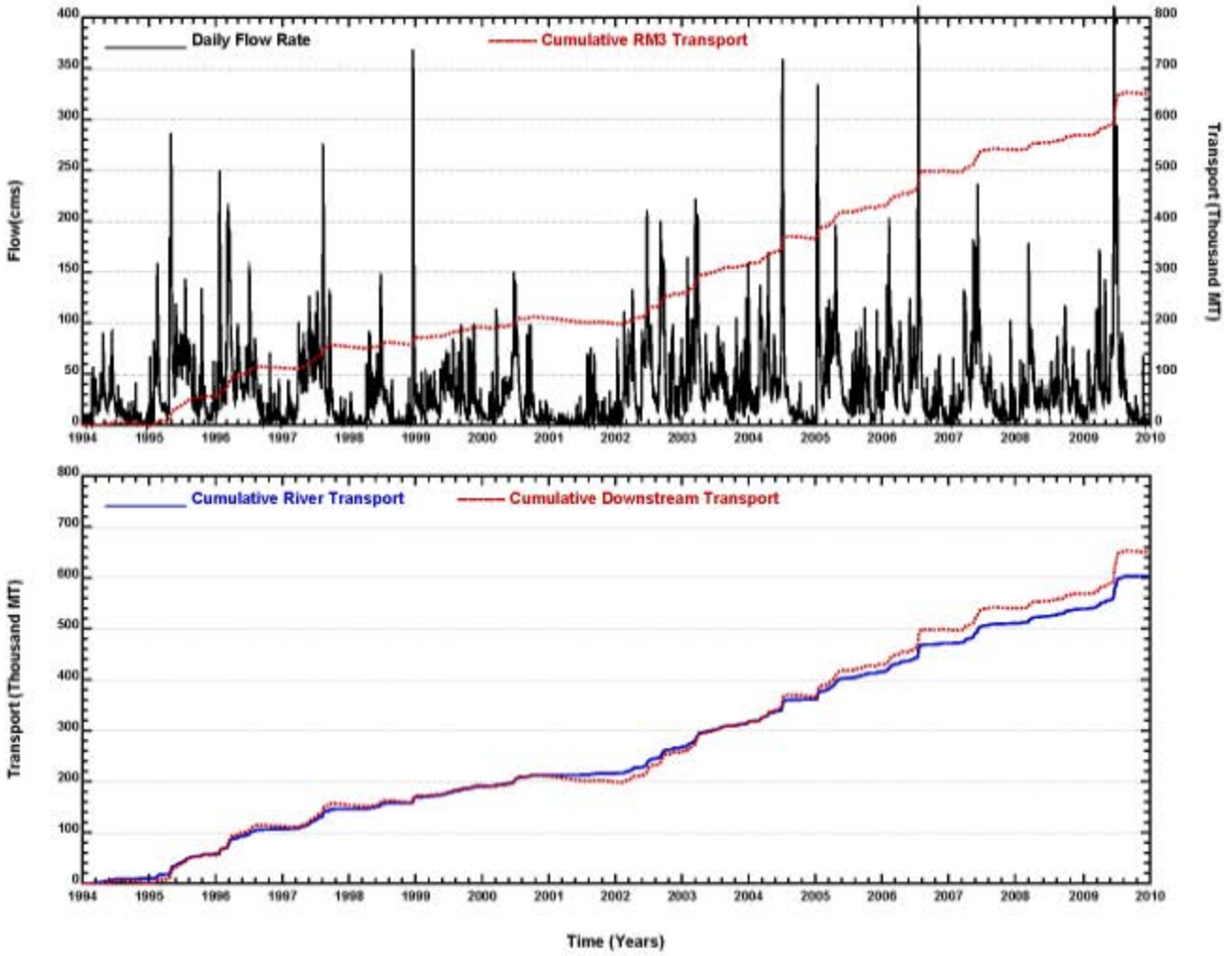

Figure 20. Flow rate and estimated cumulative transport near RMs 3 to 4.2 (top) and cumulative river input from Dundee Dam. Estimated transport near RMs 3 to 4.2 (bottom) from October 1994 through January 2010.

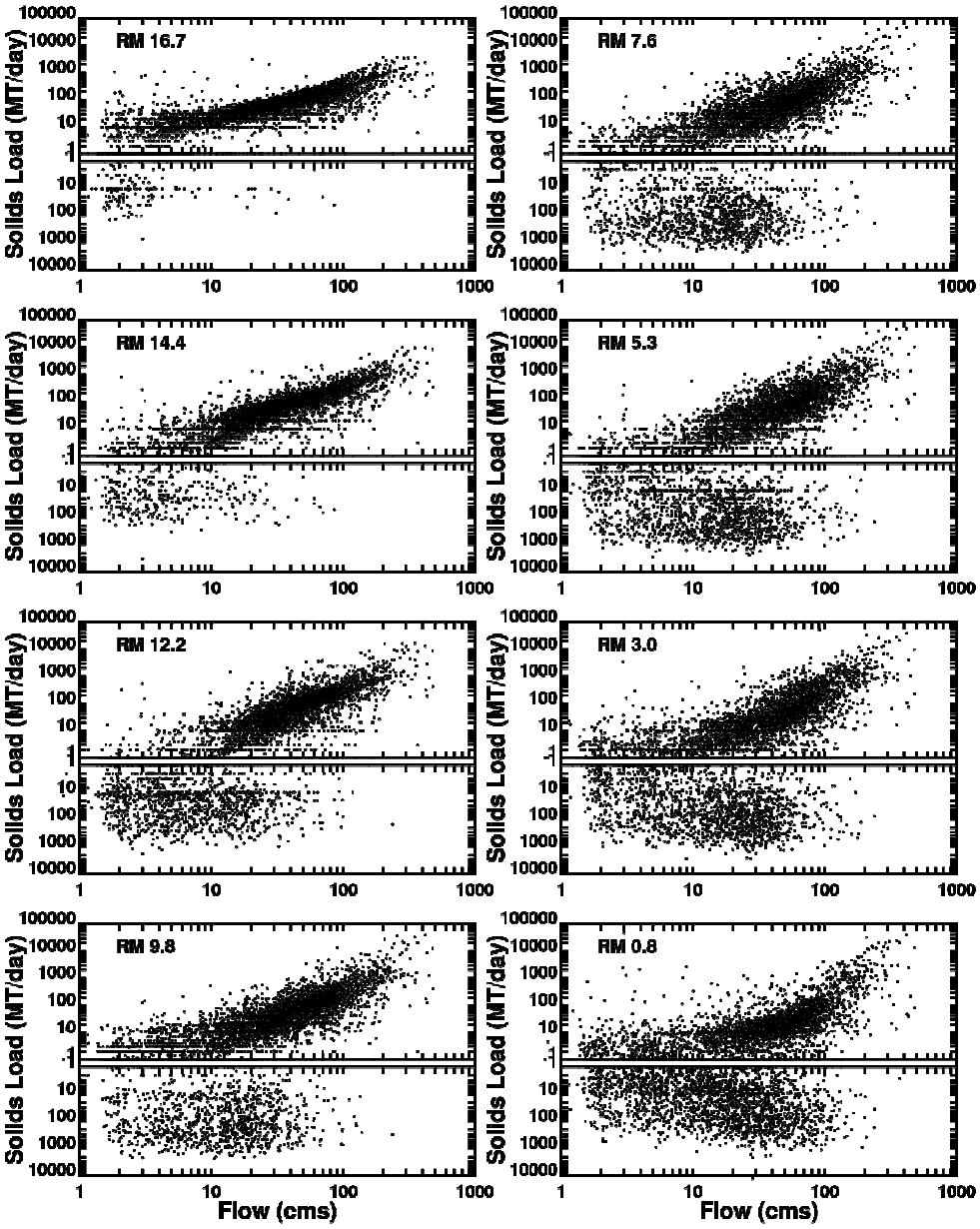

Figure 21. Daily water column sediment transport (negative is upstream) as a function of flow rate at 8 river mile stations in the Lower Passaic calculated from the preliminary HQI hydrodynamics and sediment transport model.

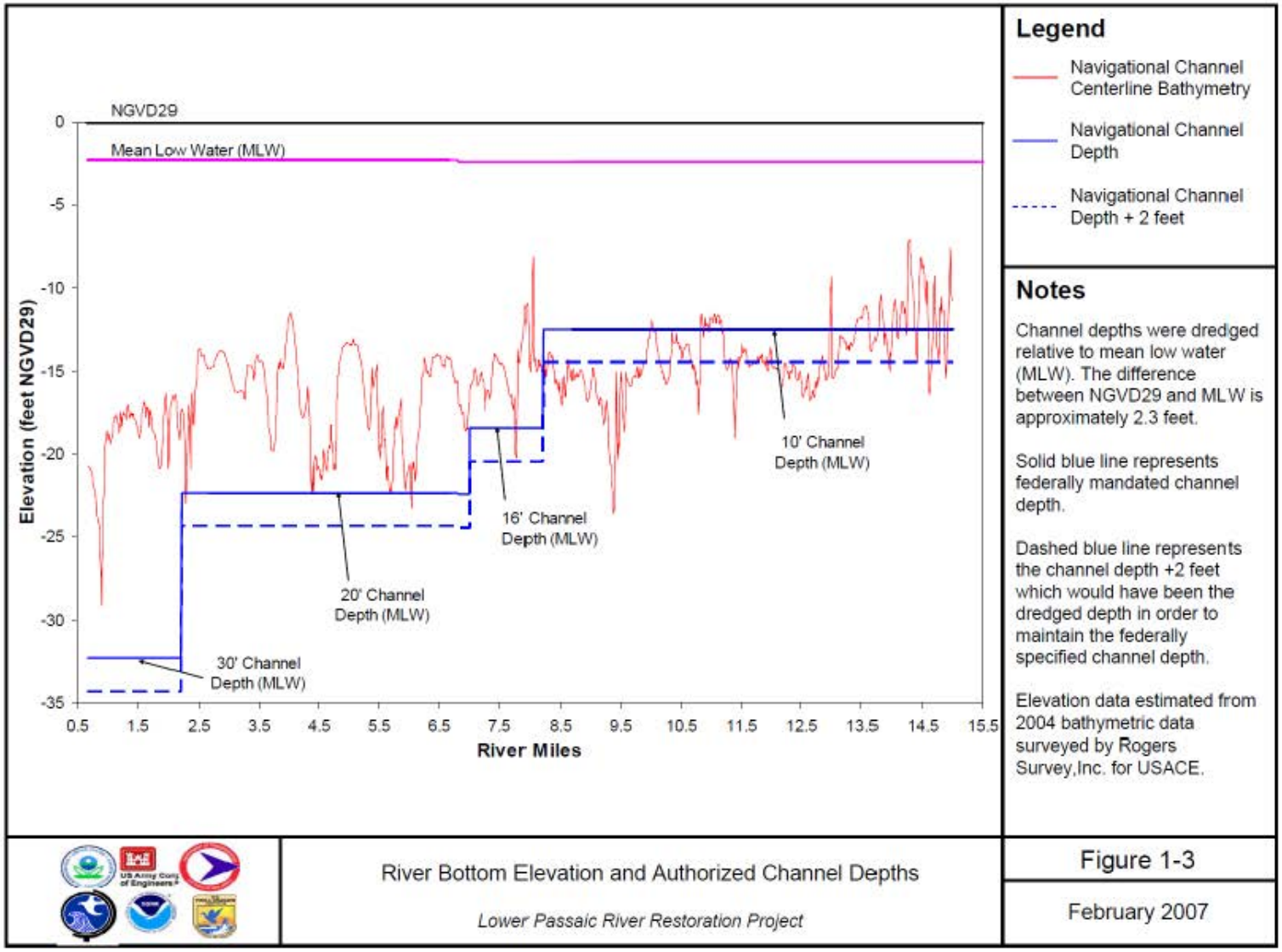

Figure 22. Depth of the river channel based on a 2004 bathymetric survey as well as the original dredged elevations as reported in USACE records (MPI, 2007).

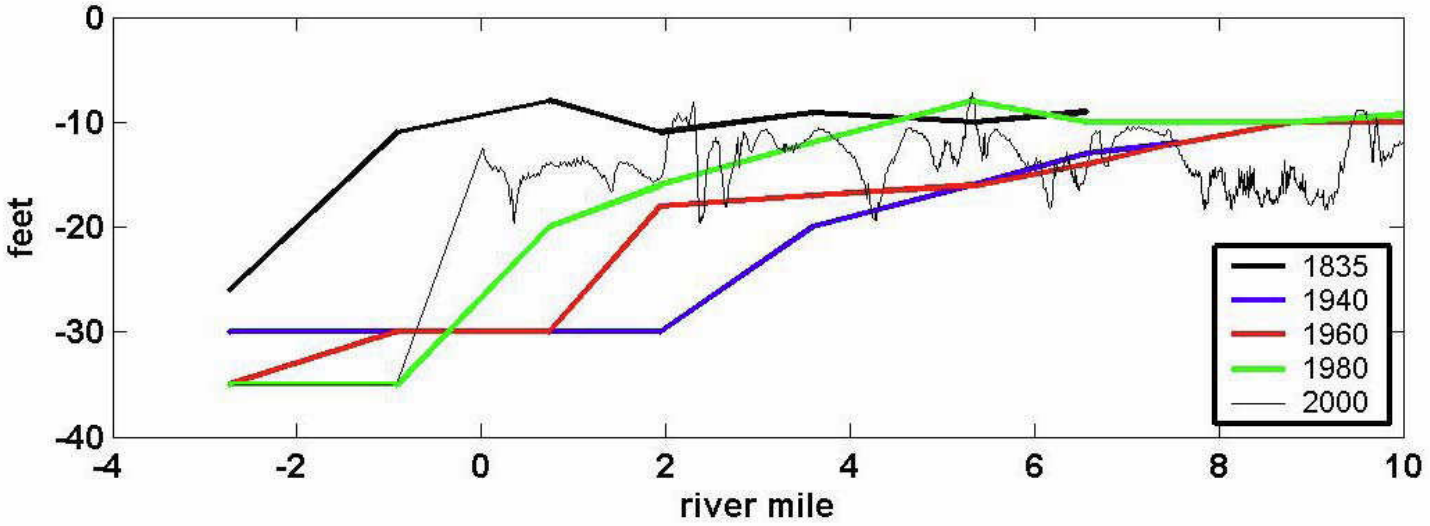

Figure 23. Estimated depths of the river channel from Chant et al. (2009).

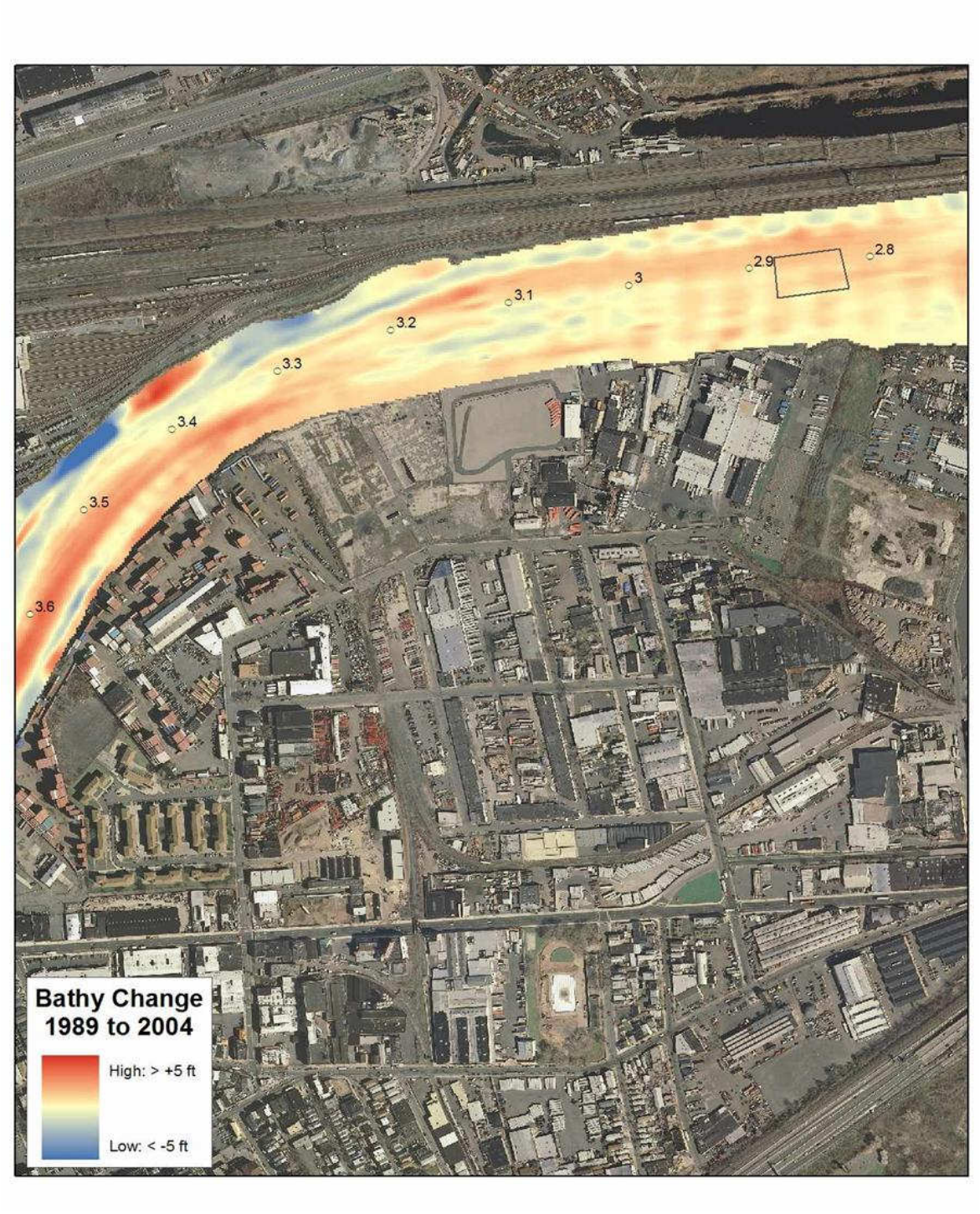

Figure 24. Bathymetric change from 1989 to 2004 from conditional simulations.

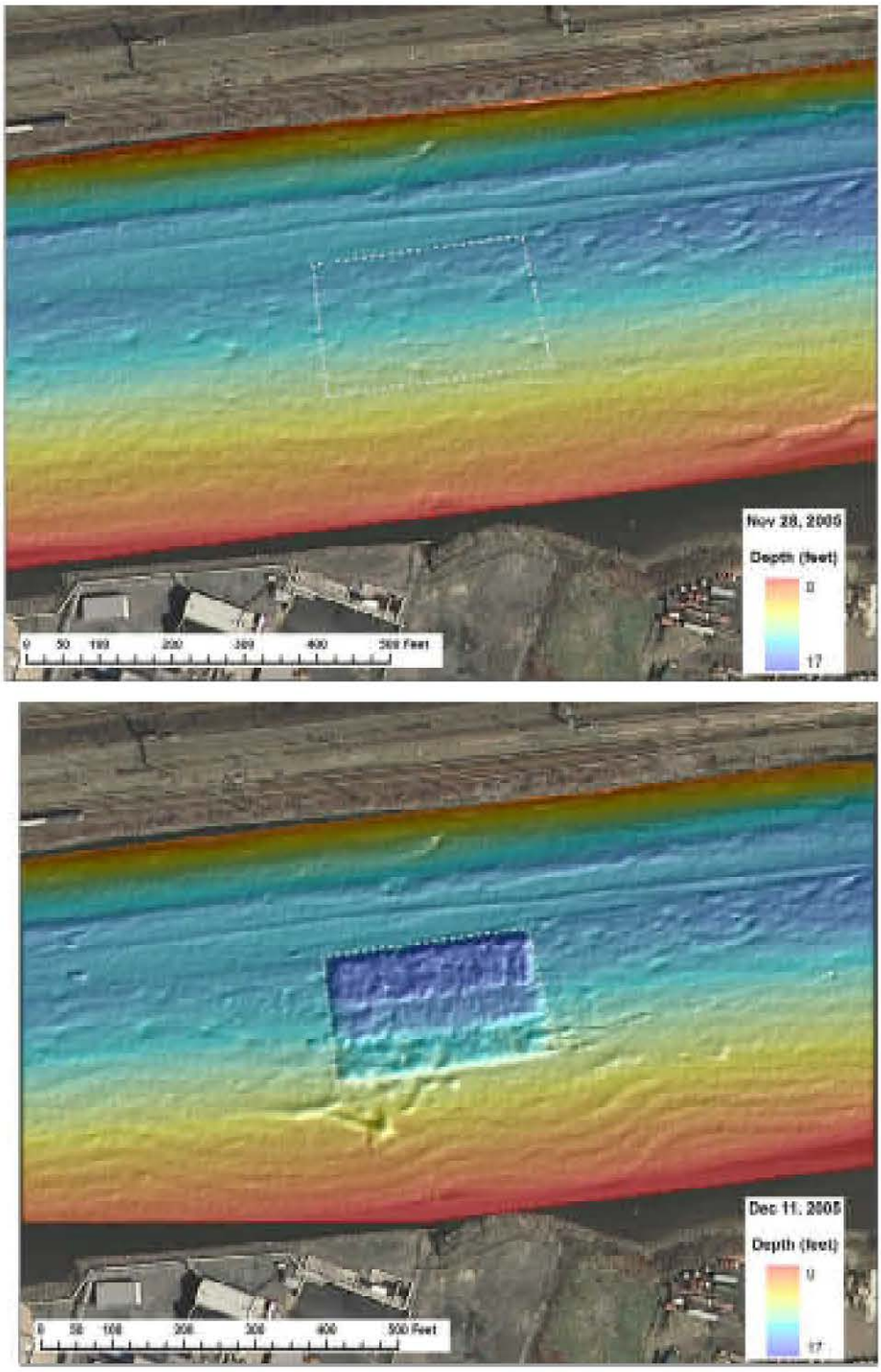

Figure 25. Pre- and Post-surveys for the 2005 pilot dredging operations.

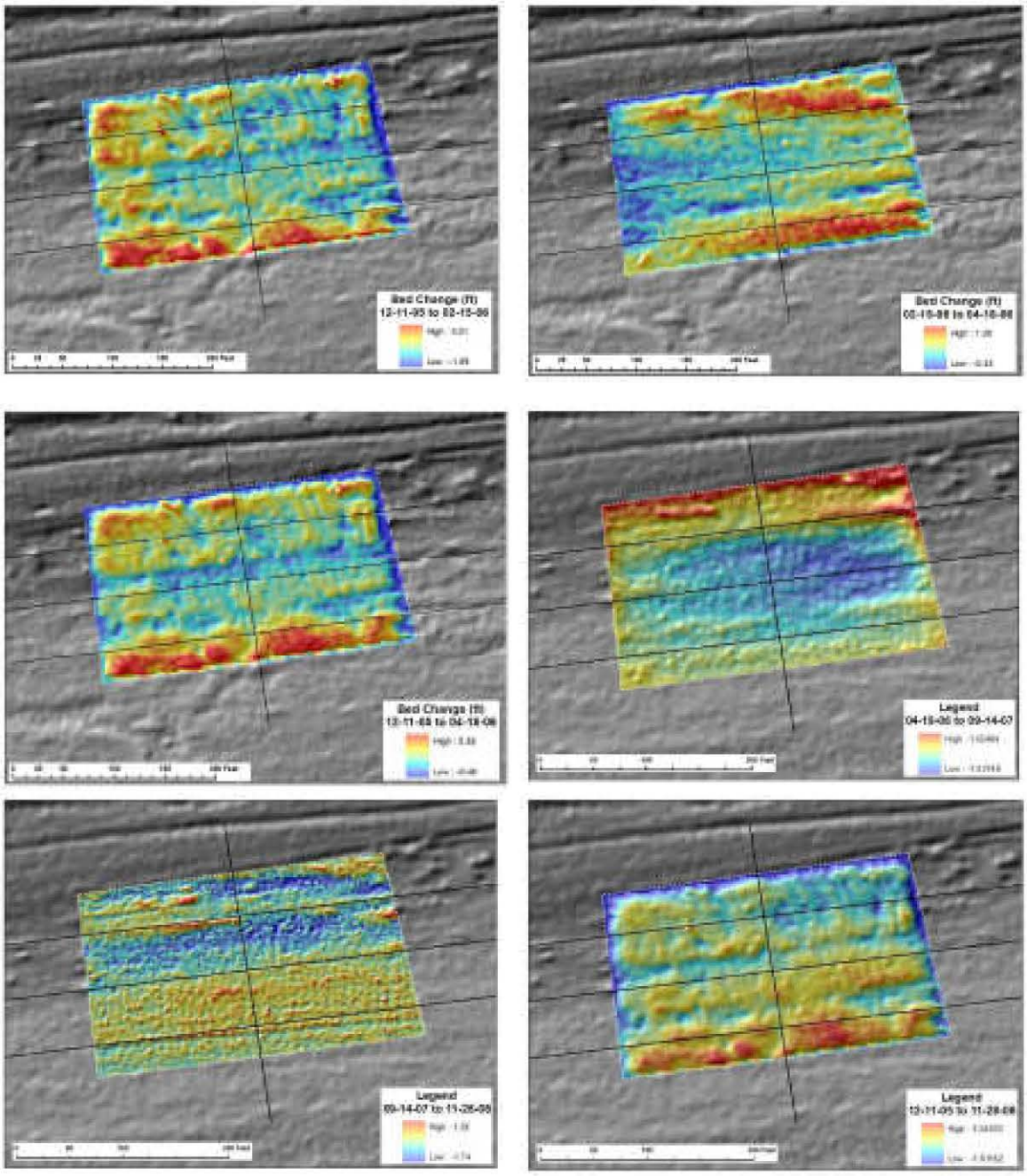

Figure 26. Net change in bed elevation following pilot dredging operations. Intervals for each change comparison are listed in the plot legend.

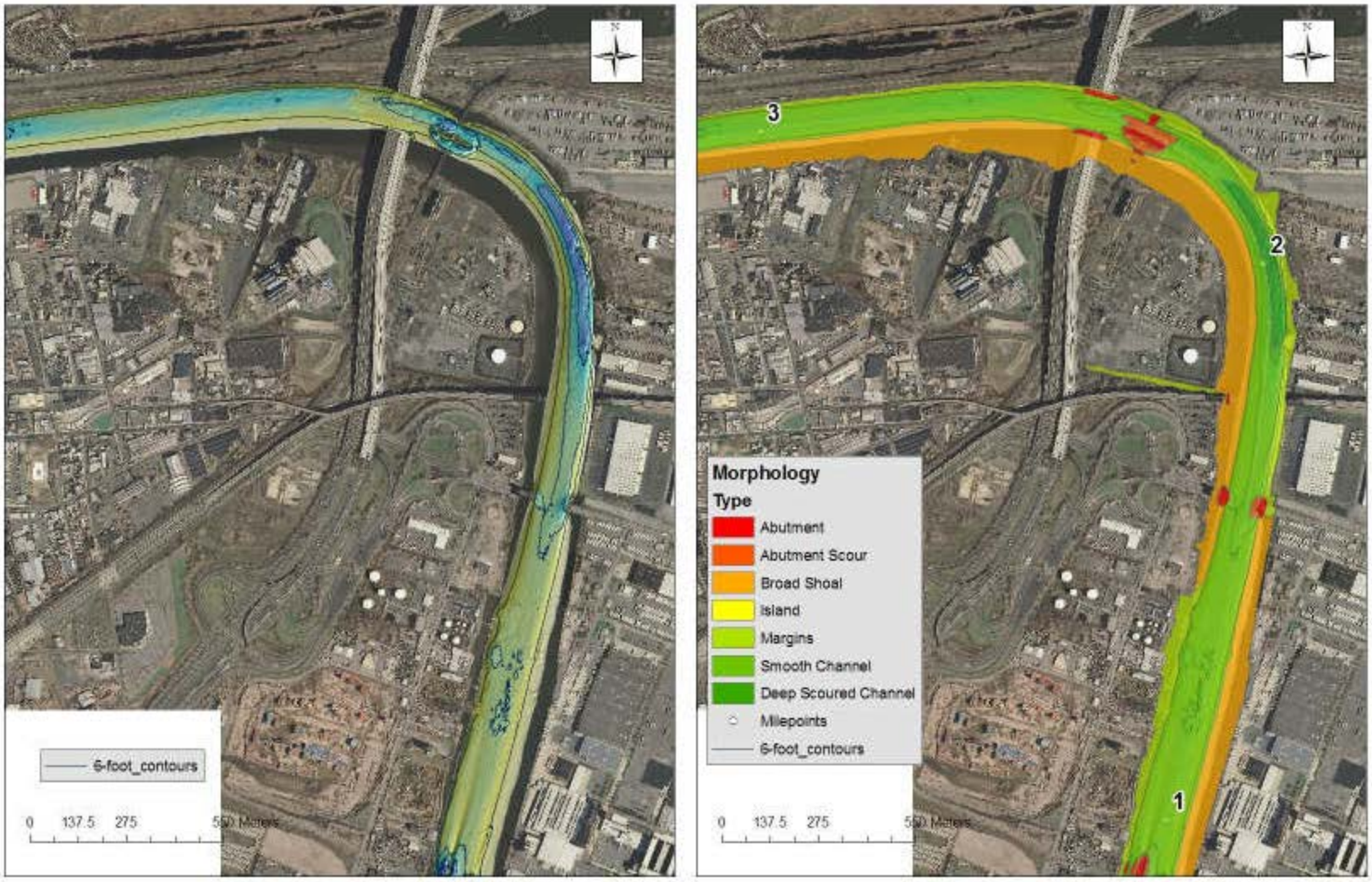

Figure 27. Shaded multibeam data and contours from the 2008 survey and an overlay of qualitatively identified morphologic regions near RM 2.

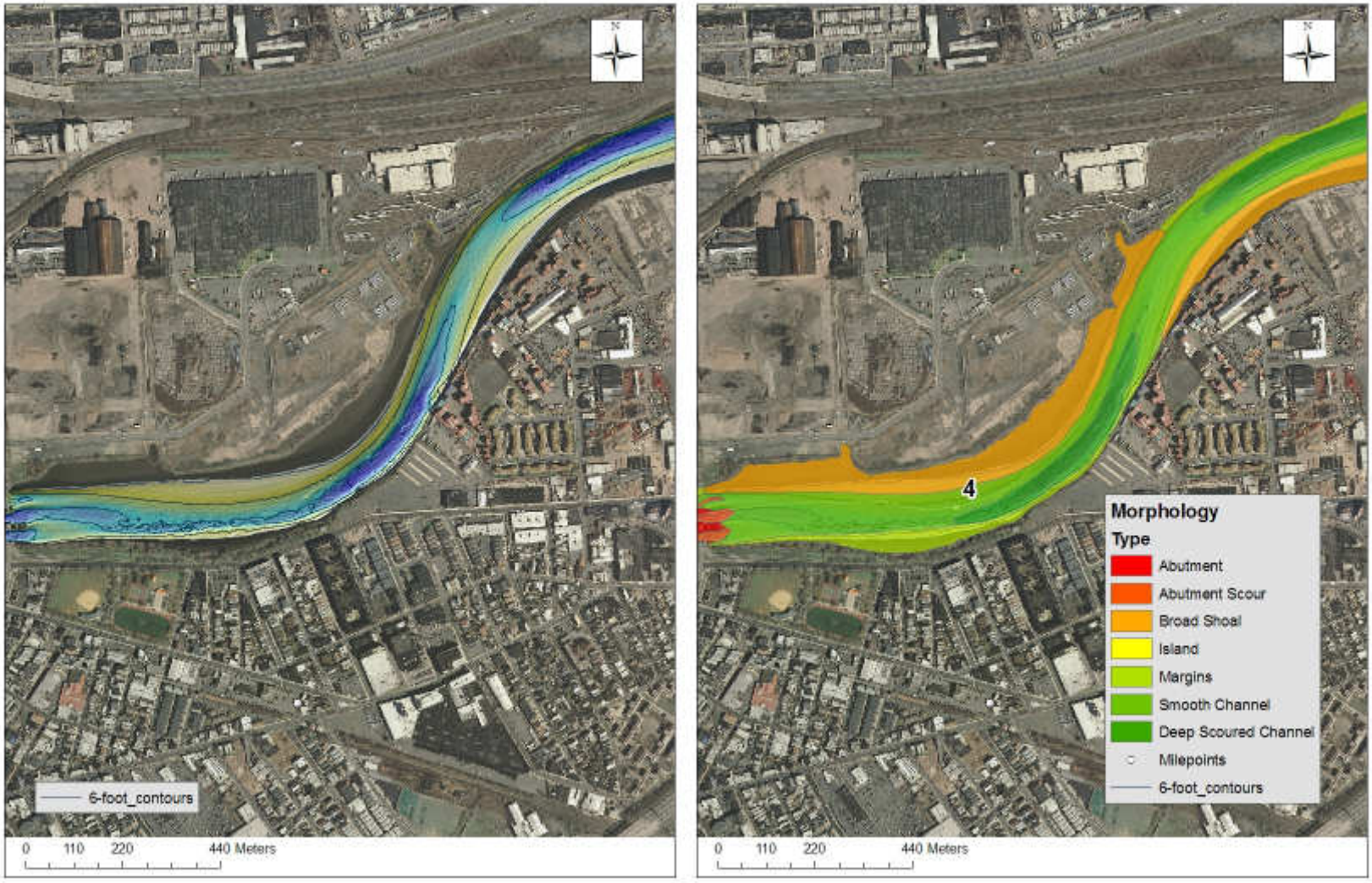

Figure 28. Shaded multibeam data and contours from the 2008 survey and an overlay of qualitatively identified morphologic regions near RM 4.

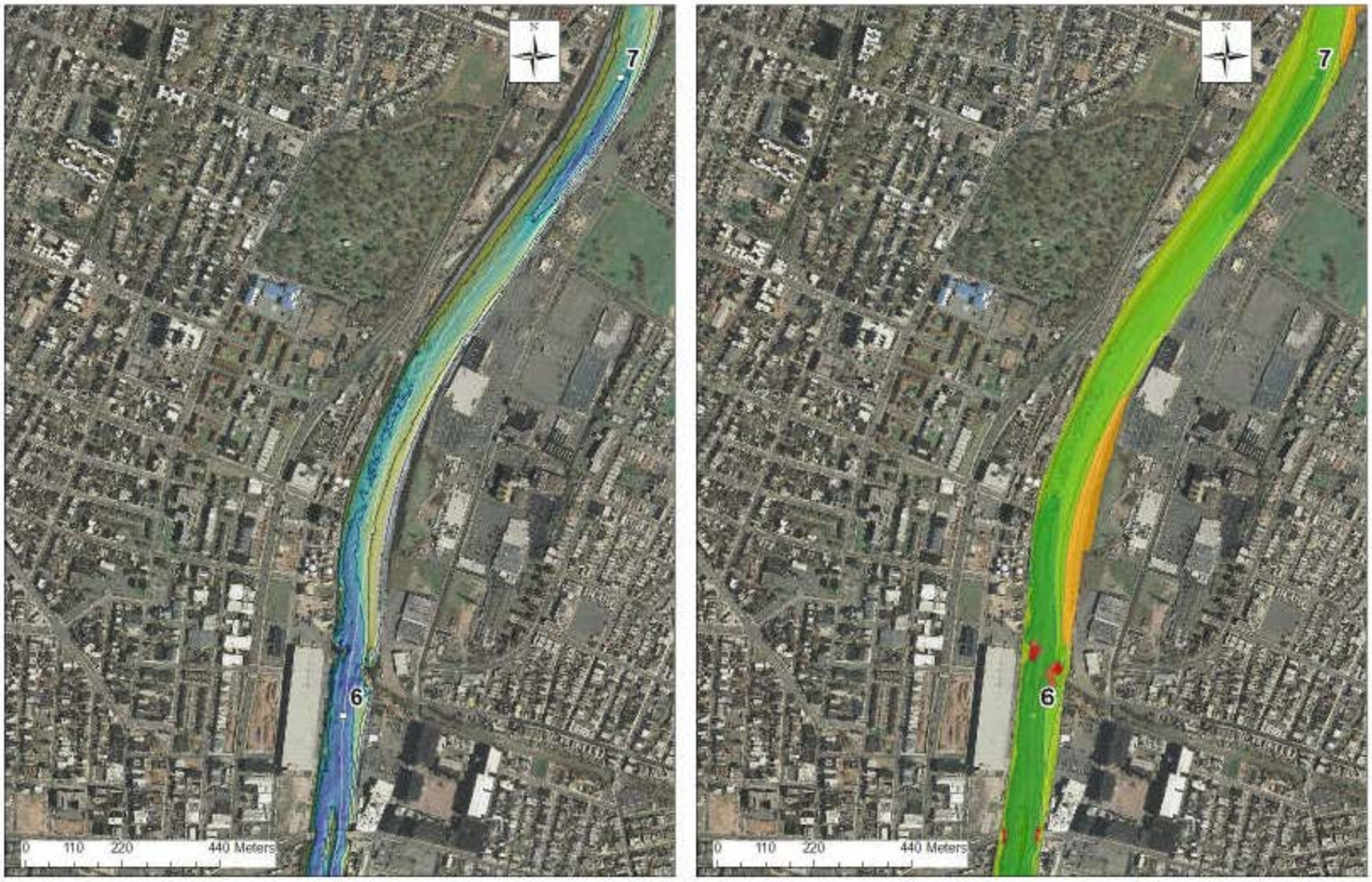

Figure 29. Shaded multibeam data and contours from the 2008 survey and an overlay of qualitatively identified morphologic regions near RM 6.

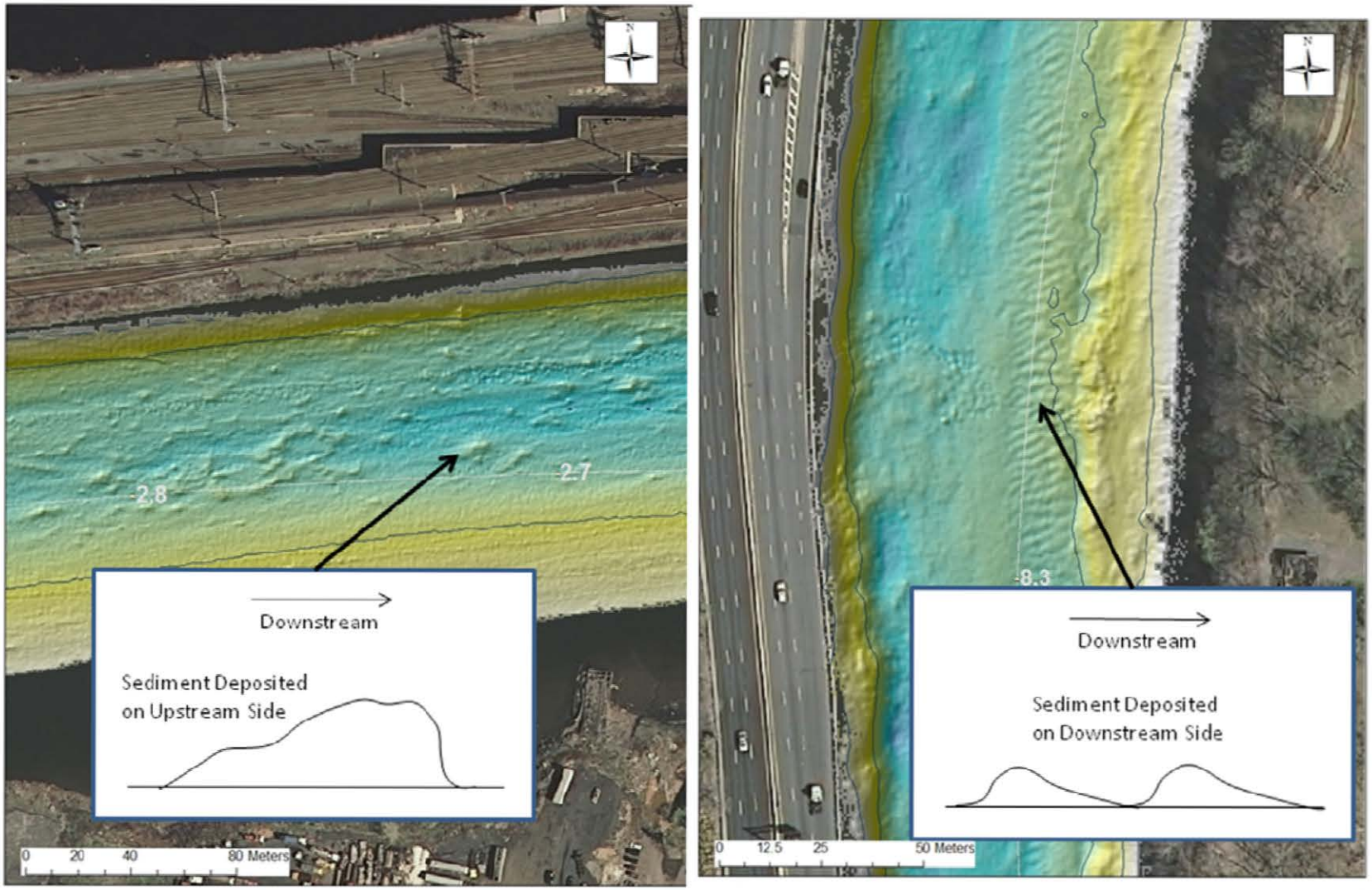

Figure 30. Shaded multibeam data from the 2008 survey highlighting bed features near RM 2.7 (left) and RM 8.3 (left).

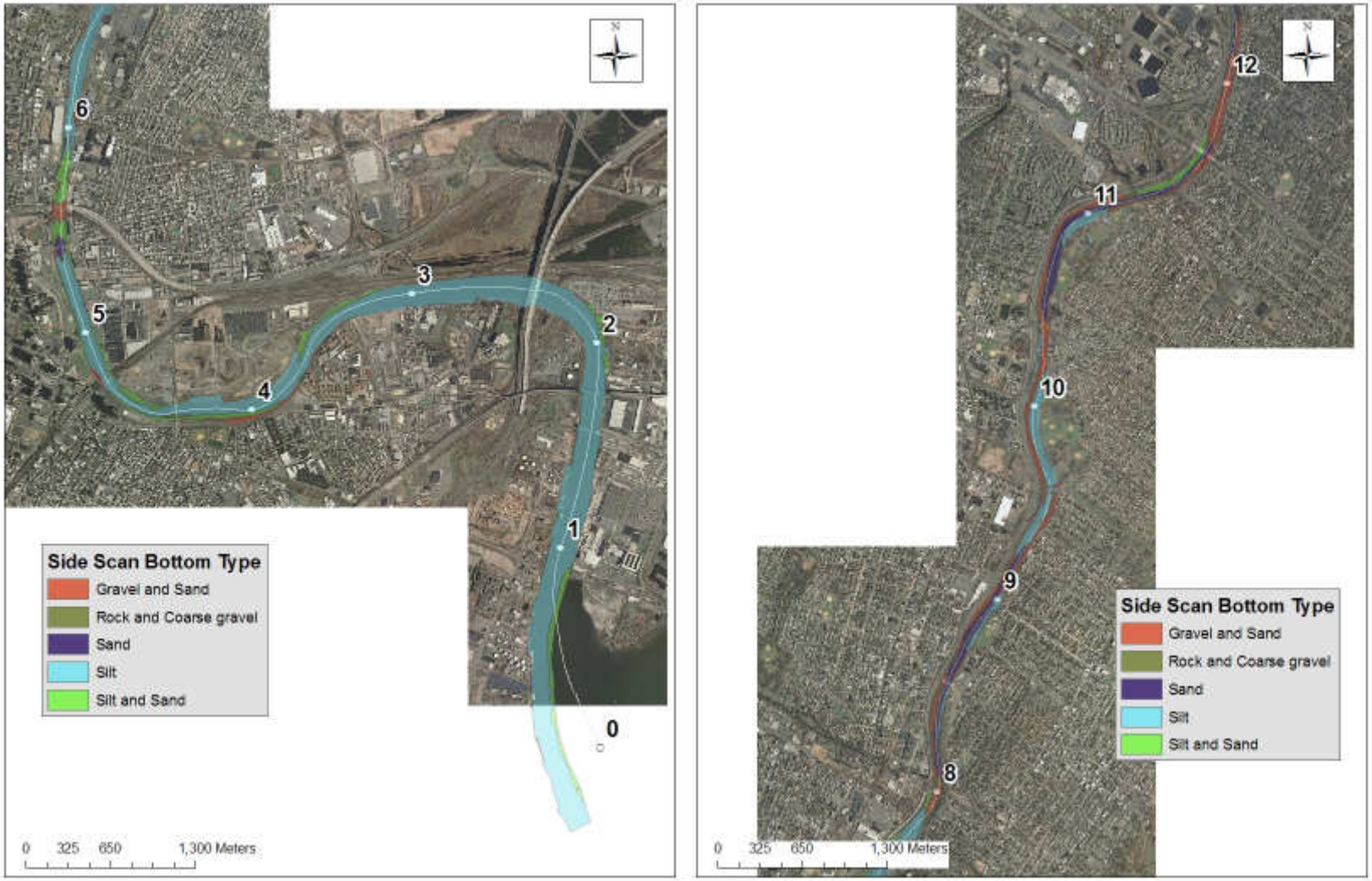

Figure 31. Side scan bottom texture identification from RM 0-6 and 8-12.

Figure 32. Side scan bottom texture identification from near RM 8.

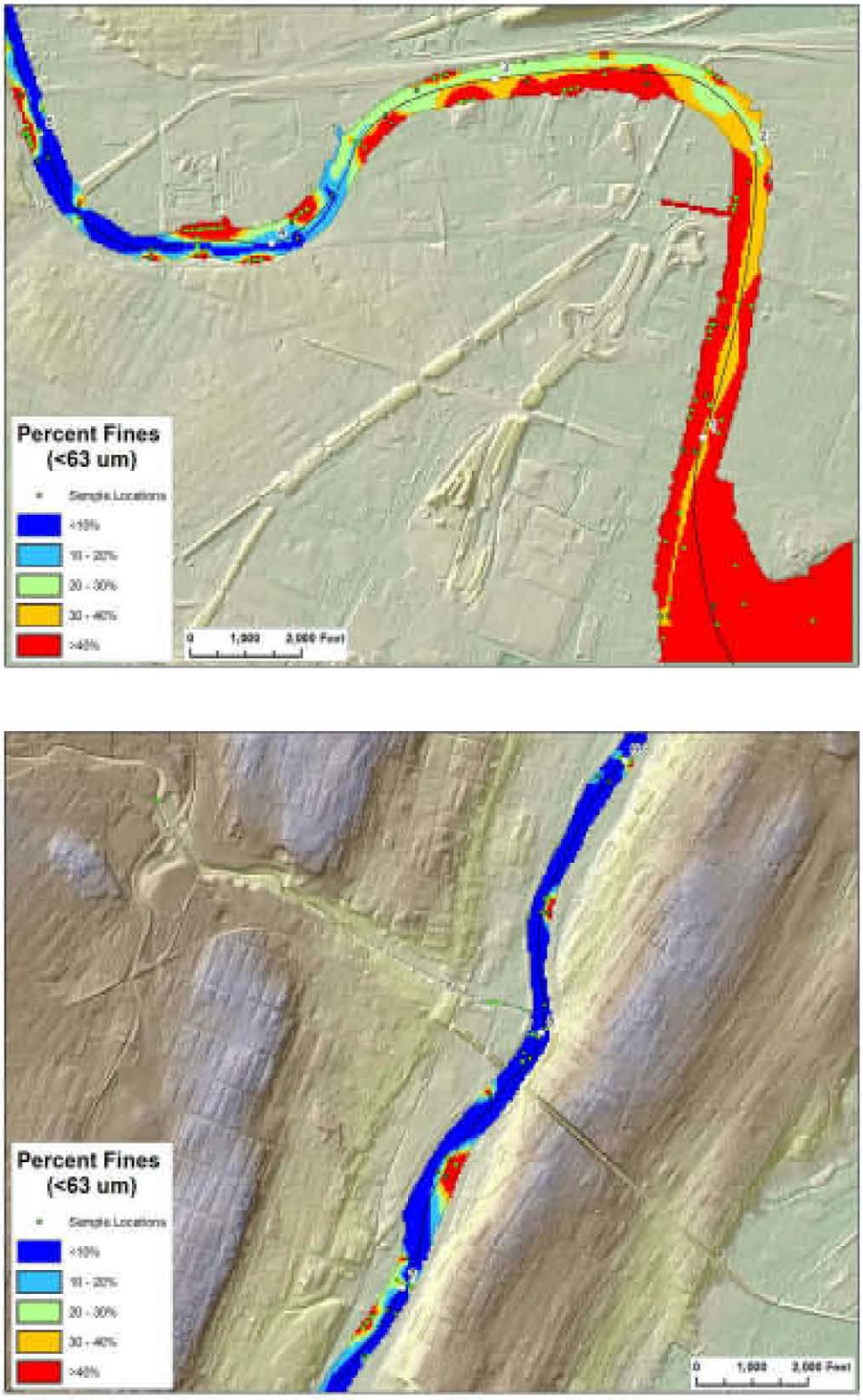

Figure 33. Interpolated surfaces of percent fines developed from the 2005 and 2008 surface sediment samples.

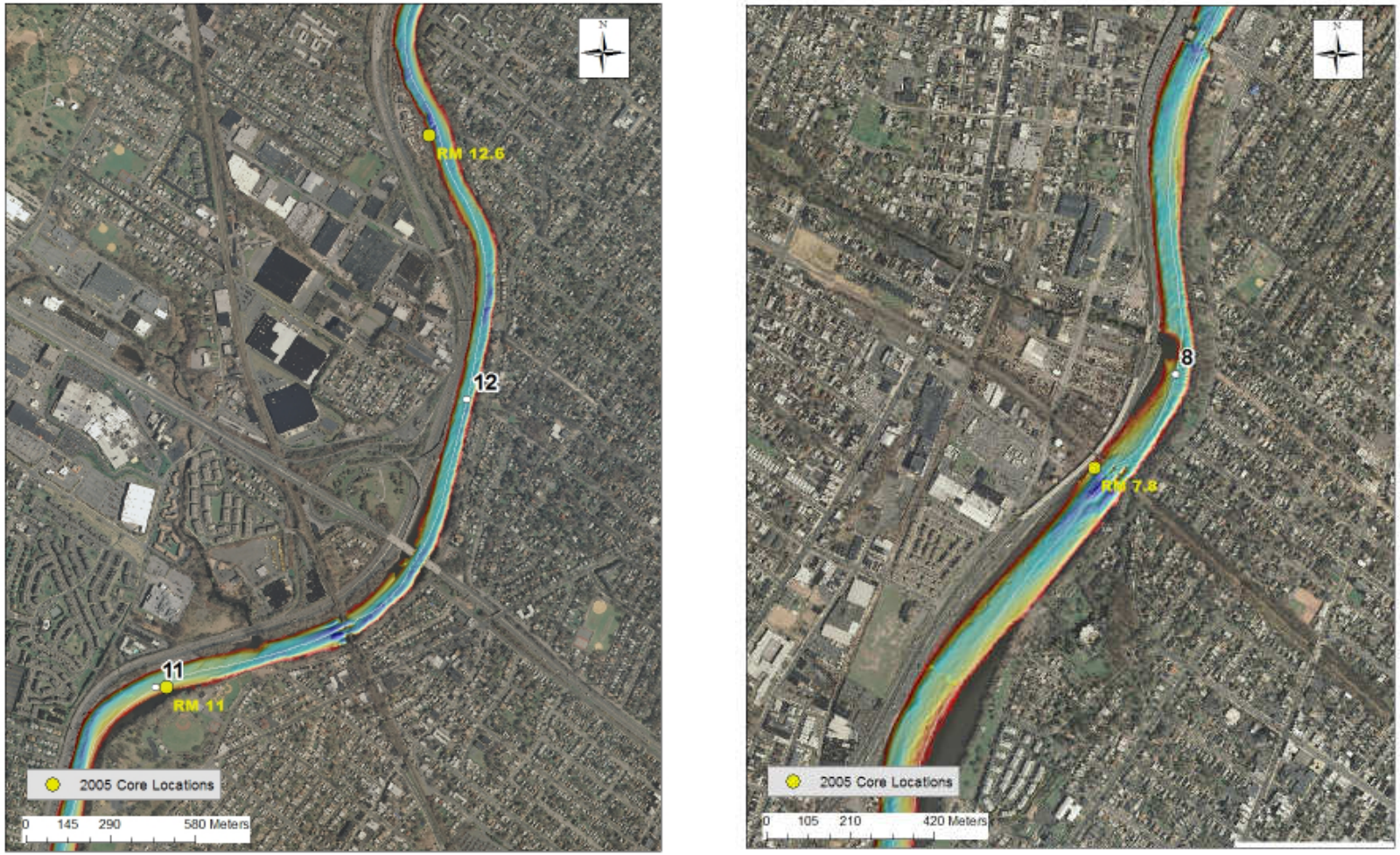

Figure 34. Locations of the three upper river 2005 CSM cores.

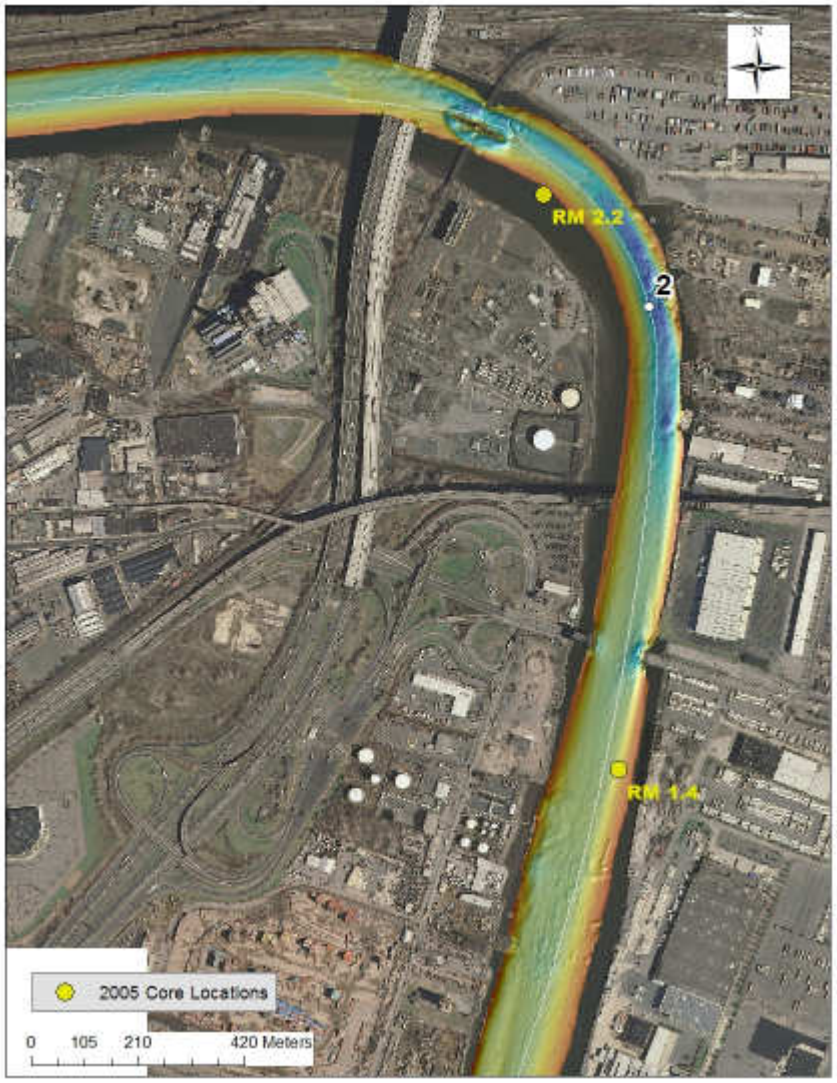

Figure 35. Locations of the two lower river 2005 CSM cores.

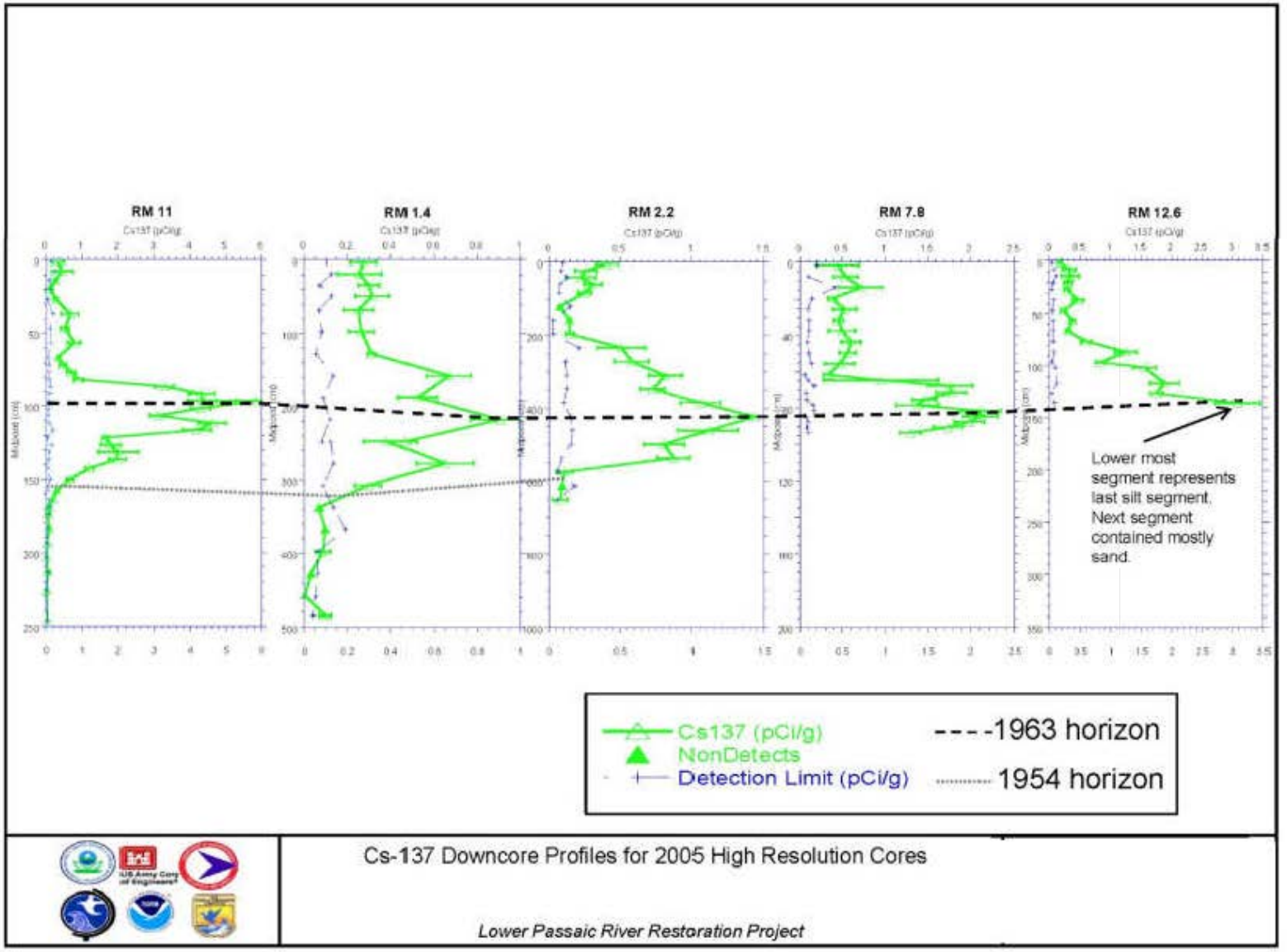

Figure 36. Profiles of Cs-137 for the 5 2005 CSM cores with 1995 PCB profiles overlain.

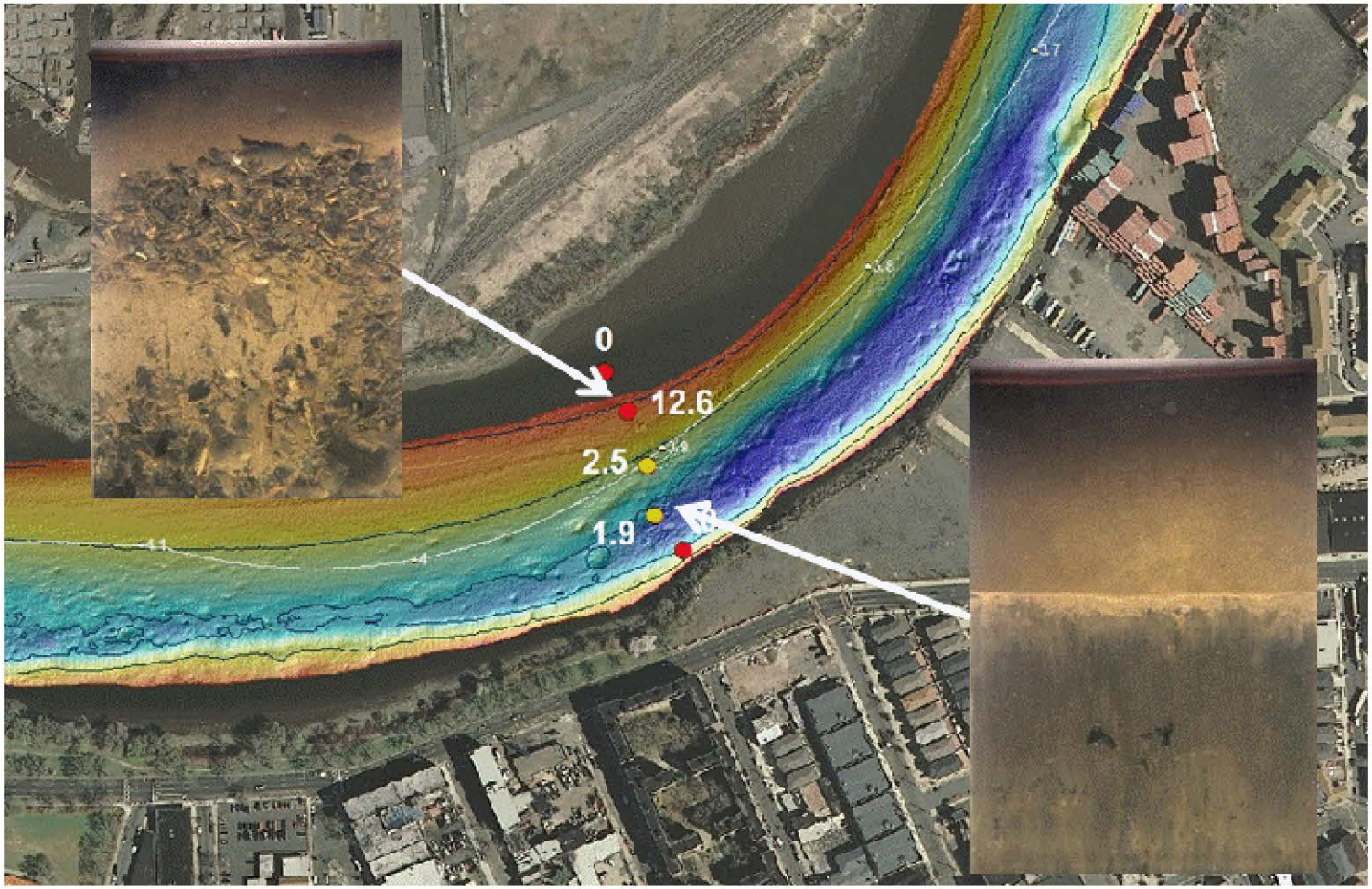

Figure 37. Shaded multibeam data from the 2008 survey and SPI camera deposition depths with photos at RM 3.9.

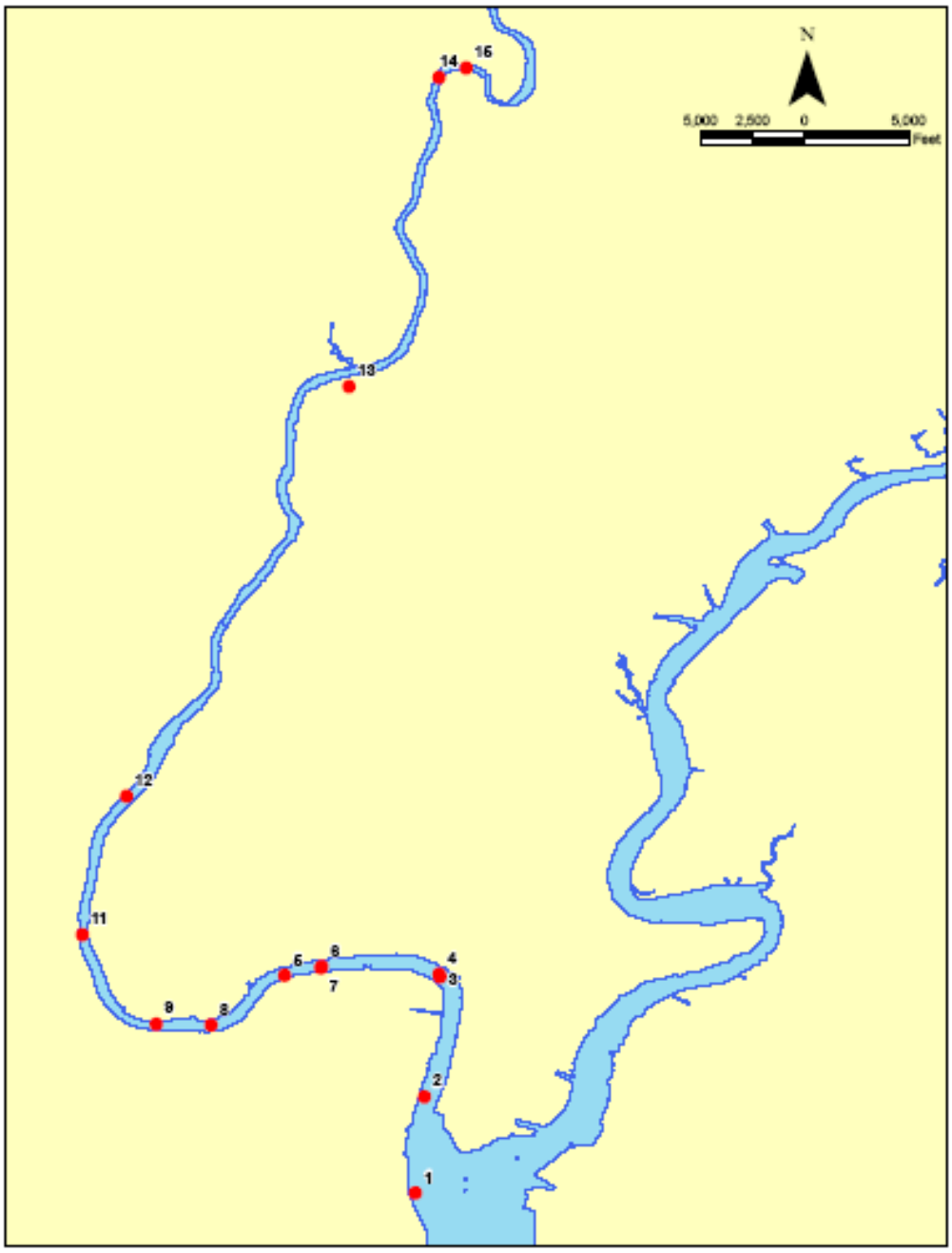

Figure 38. Map of 16 Sedflume core locations on the LPR. Note that two collocated cores were collected within ~10m of each location.

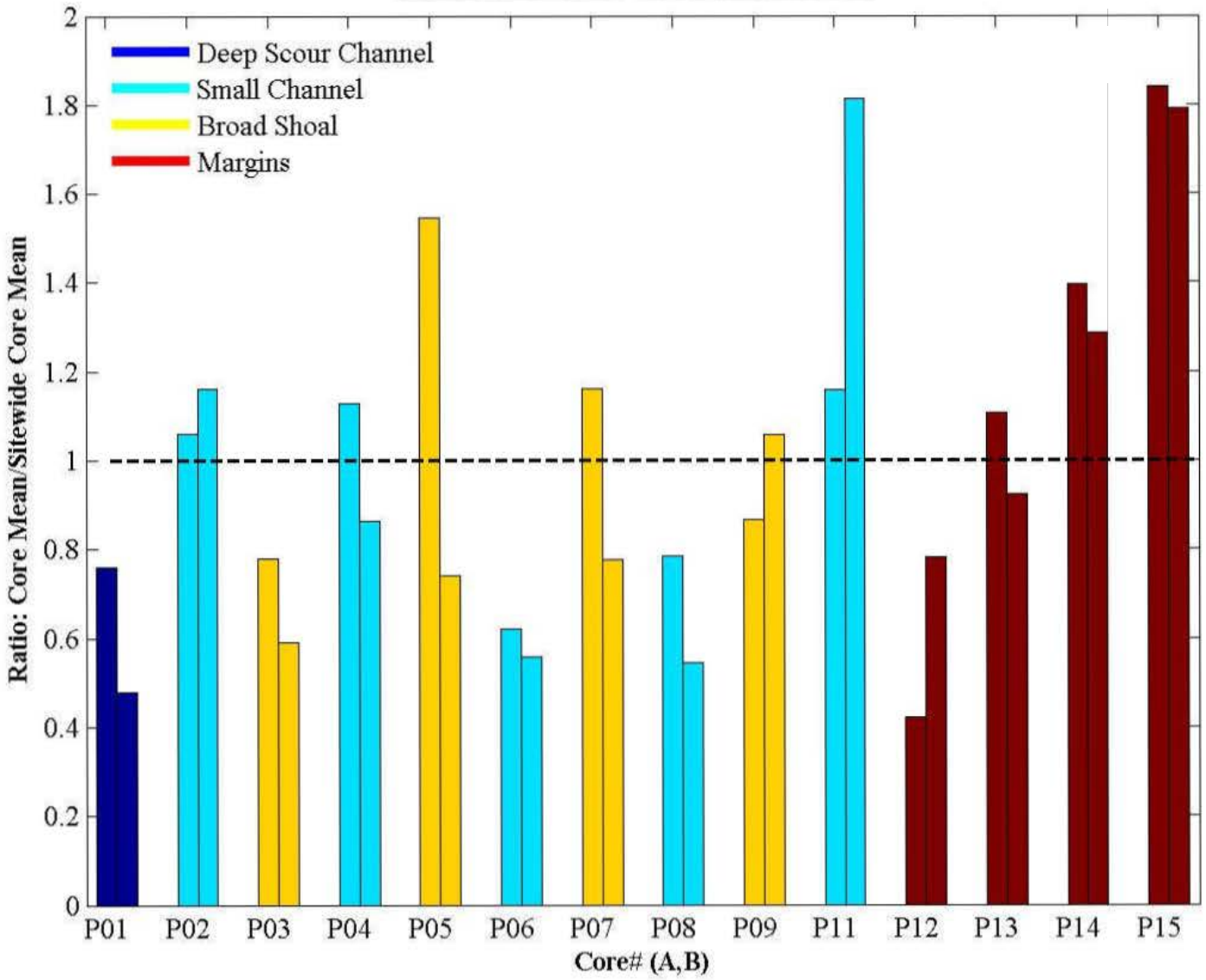

Figure 39. Average sediment erosion rate ratios for Sedflume core locations P01 through P15 colored by morphologic regions.

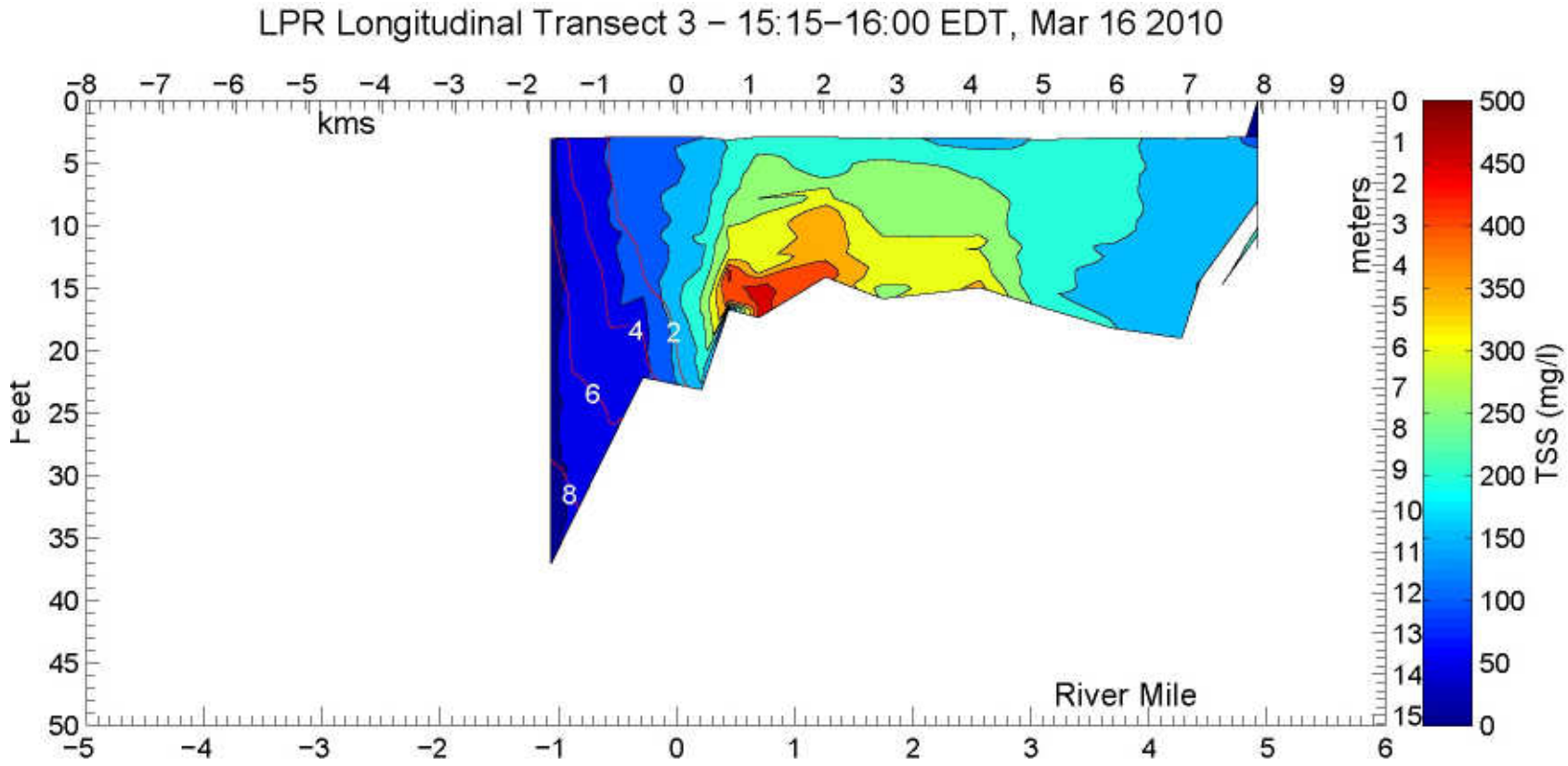

Figure 40. Longitudinal cross section of TSS derived from measurements by R. Chant during the March 16, 2010 high flow event.

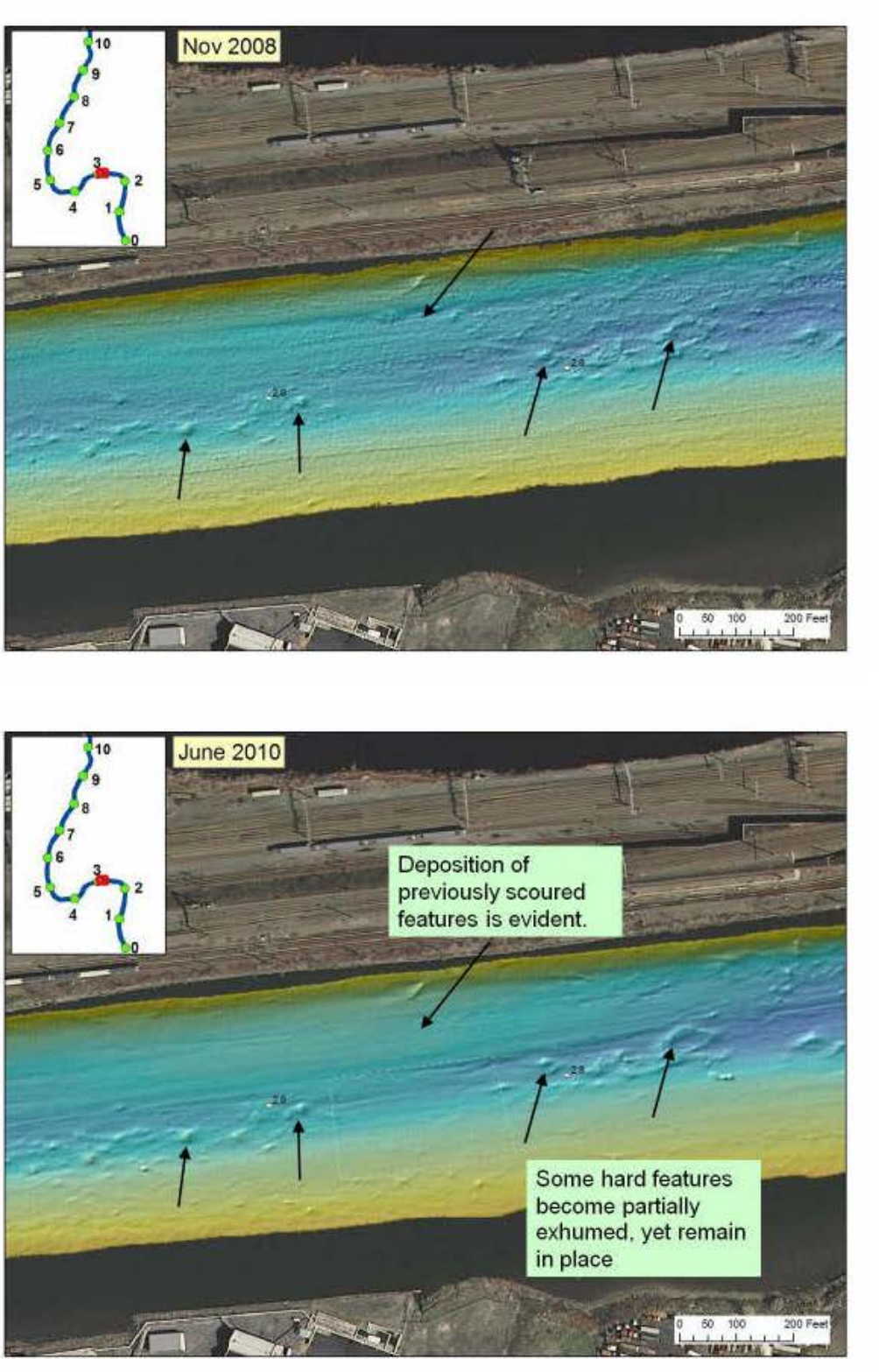

Figure 41. Comparison of channel features in the 2008 and 2010 multibeam datasets in the vicinity of the pilot dredge region.

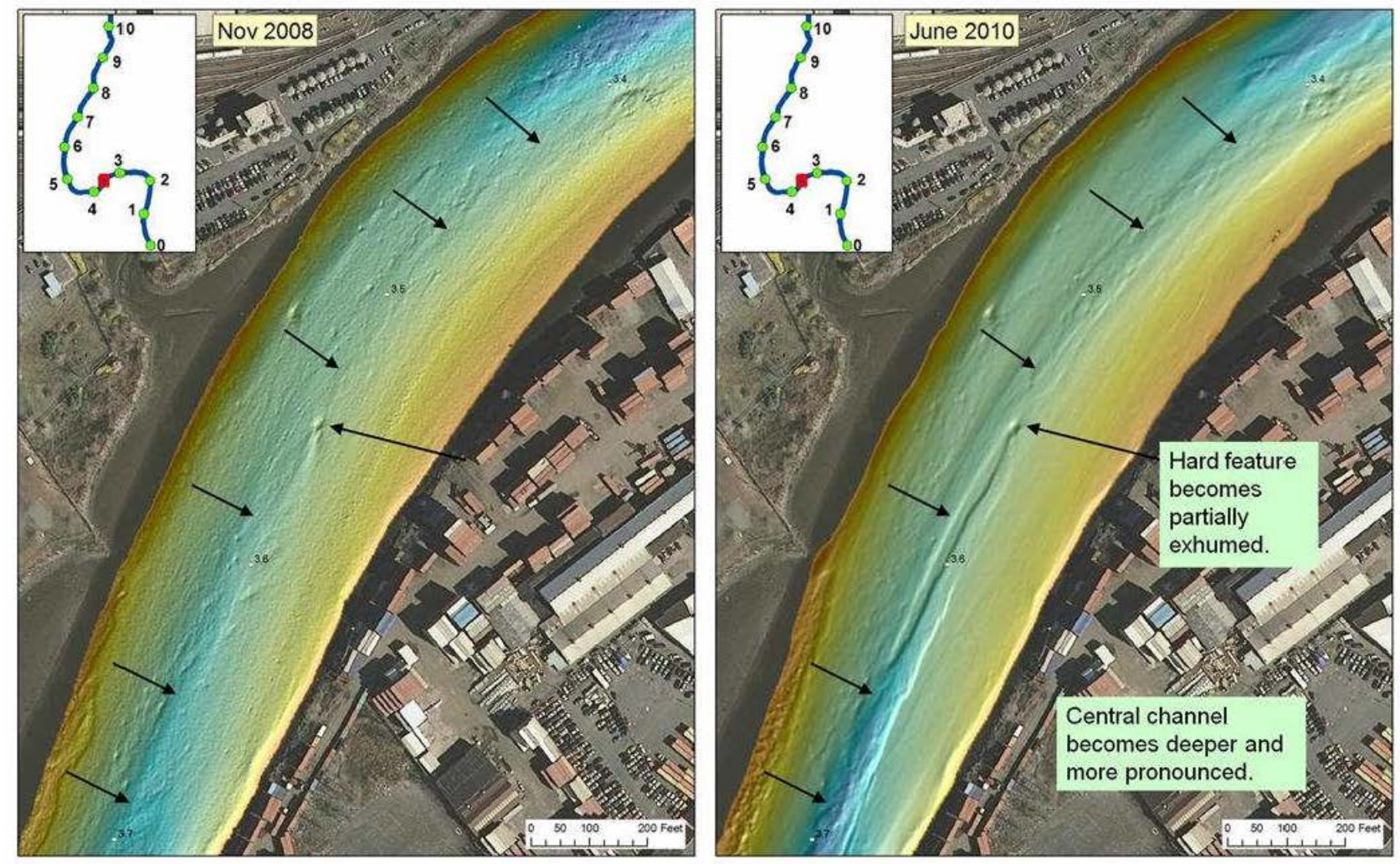

Figure 42. Comparison of channel features in the 2008 and 2010 multibeam datasets.

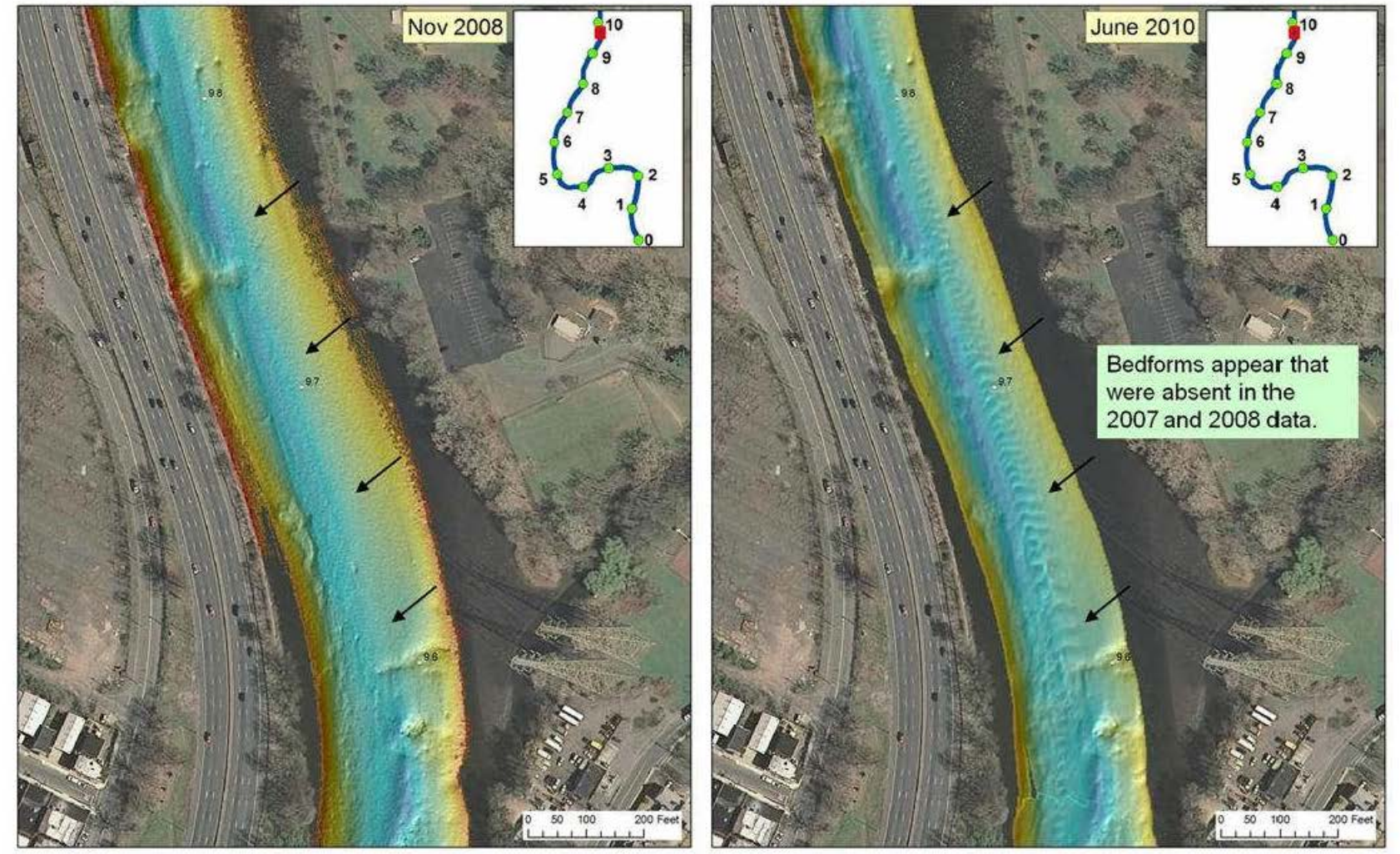

Figure 43. Comparison of channel features in the 2008 and 2010 multibeam datasets. The figure shows the evolution of bedforms.

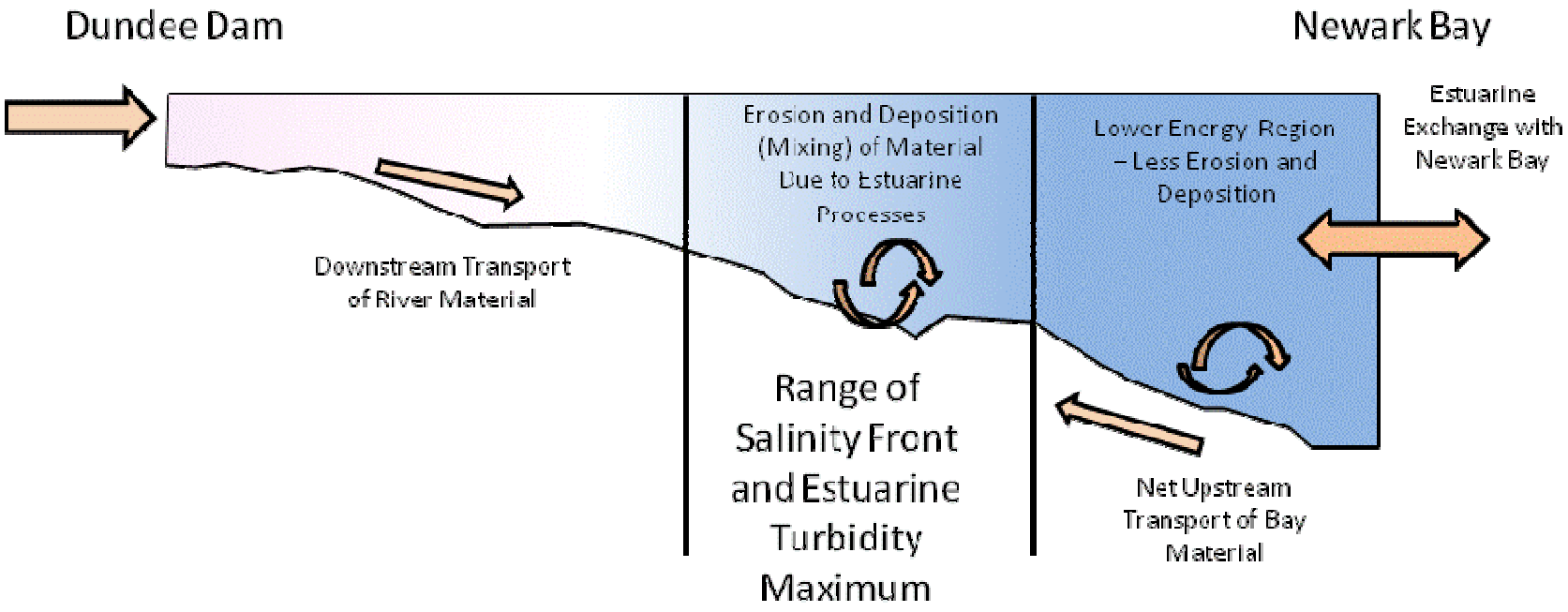

Figure 44. Conceptual diagram of key processes during low river flow conditions.

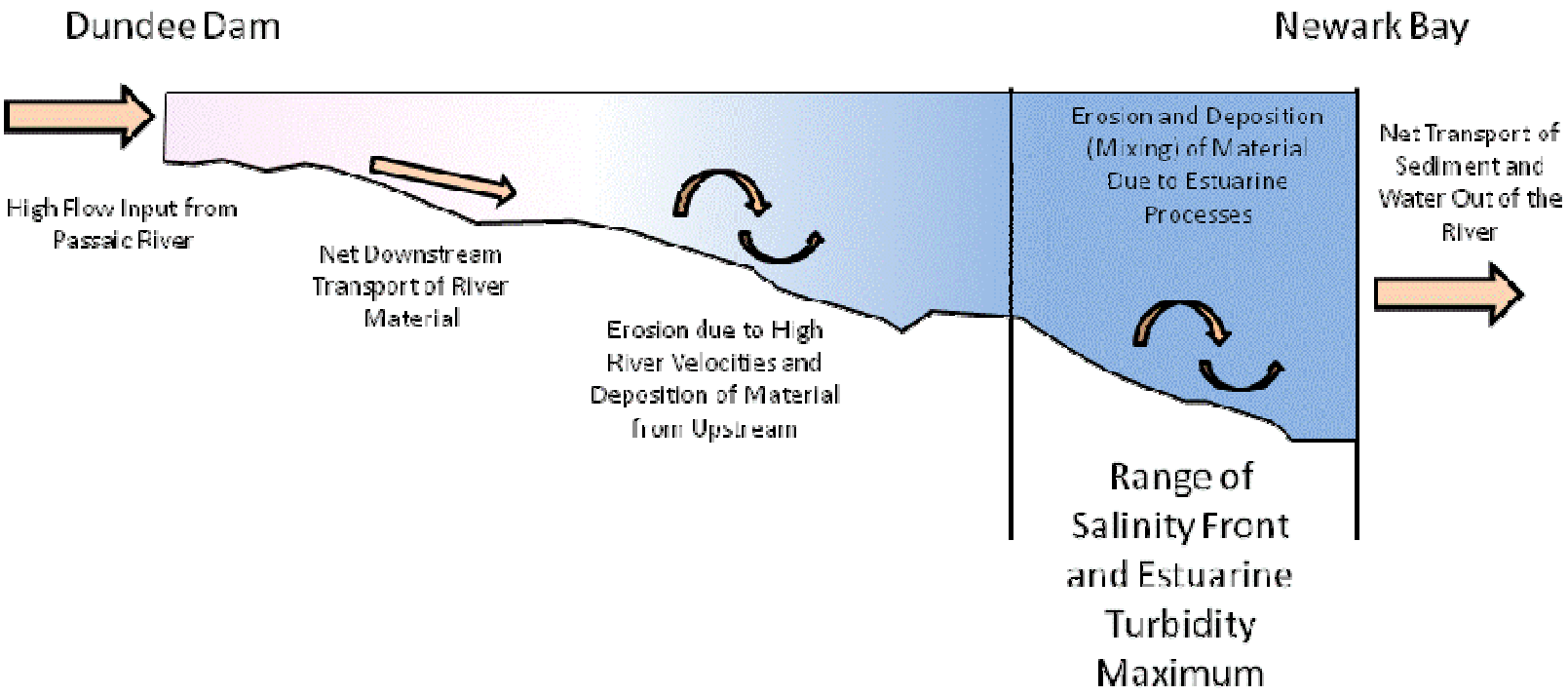

Figure 45. Conceptual diagram of key processes during high river flow conditions.